1986

System reliability assessment with nonlinear finite element analysis

H. S. Gopalakrishna
Iowa State University

8615050

Gopalakrishna, H. S.

SYSTEM RELIABILITY ASSESSMENT WITH NONLINEAR FINITE ELEMENT ANALYSIS

Iowa State University PH.D. 1986

University
Microfilms
International 300 N. Zeeb Road, Ann Arbor, MI 48106

System reliability assessment with

nonlinear finite element analysis

by

H. S. Gopalakrishna

A Dissertation Submitted to the

Graduate Faculty in Partial Fulfillment of the

Requirements for the Degree of

DOCTOR OF PHILOSOPHY

Department: Civil Engineering
Major: Structural Engineering

Approved:

Signature was redacted for privacy.

In Charge of Major Work

Signature was redacted for privacy.

For the Major Department

Signature was redacted for privacy.

For the Graduate College

Iowa State University
Ames, Iowa

1986

TABLE OF CONTENTS

LIST OF FIGURES

LIST OF TABLES

1. INTRODUCTION

1.1. General

In traditional design practice, the structural parameters such as material properties and dimensions are considered as specific constants. When analyzed for a given set of loads the behavior is concluded to be deterministic. In reality, the strength and load parameters show variation in their values. For example, a repeated number of tests of concrete strength specimens from the same source show a set of different values. Other examples of such structural parameters are the cross sectional dimensions, yield strength of steel, the elastic modulus, and live loads on the structure. Data on these parameters exhibit statistical variation. For example, the elastic modulus of steel can be statistically described as lognormally distributed with a coefficient of variation of 0.025 (4). In a structural problem, these basic parameters determine the structural behavior of load vs. displacement or stress vs. strain. Therefore, the uncertainty in basic variables introduce uncertainty and variation into the structural response. The input and output parameters in a structural model should, therefore, be considered non-deterministic and the structural problem be regarded as statistical (Figure 1).

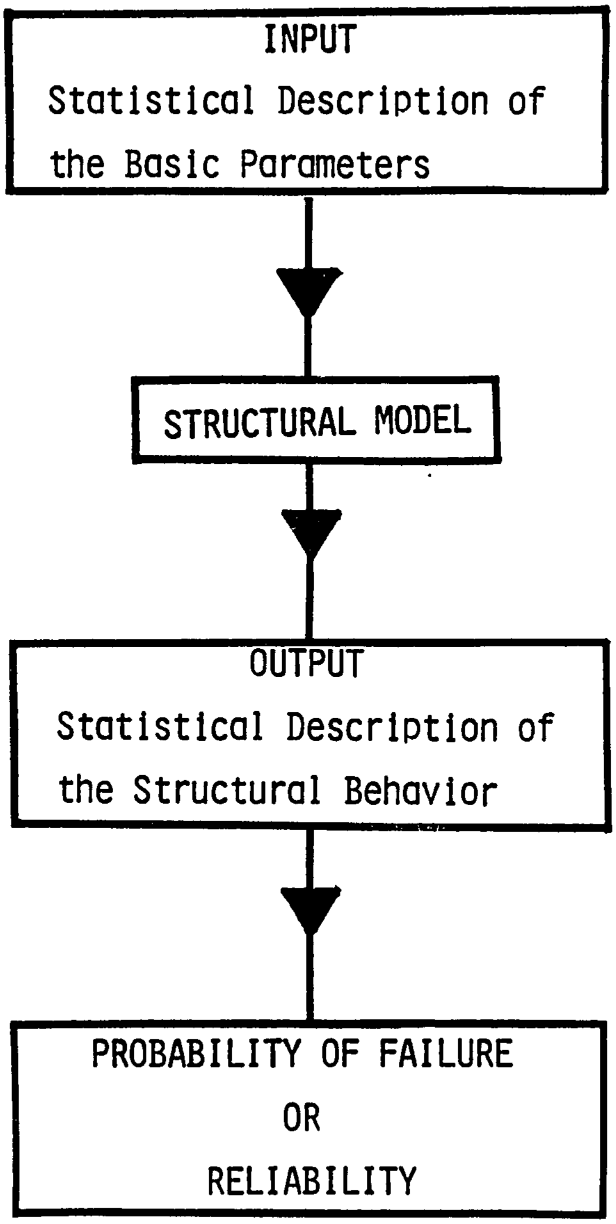

Figure 1. Structural reliability analysis.

Since the output from the structural model shows variation, the structural performance for which it is designed is uncertain. The possibility of failure is due to uncertainty in the structural performance. To understand safety and performance, a statistical approach can be taken. In this approach, the primary purpose is to evaluate the probability of failure. One minus the probability of failure is the reliability.

Application of a probabilistic approach has gained considerable attention in the field of structural engineering (6). In North America and Europe, probability based design codes have been recently introduced. In these design codes, the load and resistance factors are defined. These factors are based upon a first order probability analysis. Information regarding this is found in Construction Industry Research and Information Association (CIRIA) report (4) and National Bureau of Standards (NBS) report (9). Probabilistic methods also play an important role in making rational comparisons between alternative designs (3, 9). Other areas of application include the evaluation of the reliability of existing structures (27) and the estimation of the risk of nuclear power plant structures (32).

1.2. Problem Definition

The outline of the structural reliability problem is shown in Figure 1. The structural model is the link between the basic parameters and the structural behavior. For simple structures, the structural model can be represented by an expression. For example, let the load, elastic modulus and moment of inertia be the basic variables in a simply supported beam. If the maximum deflection is of interest, then an expression for the maximum deflection can be obtained in terms of the above parameters. This expression is regarded as the structural model. In such a simple situation, classical reliability methods can be used in relating the statistics of the basic parameters to the statistics of the maximum deflection. The probability that the deflection would exceed certain limits can then be evaluated.

In practical situations, the structure is composed of several components. The main concern in such a system is not the failure of a component but the overall system failure. In such practical cases, the description of the structural model by an explicit expression is extremely difficult. However, numerical techniques such as the finite element method can be used to determine the structural behavior.

In most structural cases, deformation is an appropriate measure of behavior. The structure is regarded as failed if the deflection (U_Q) reaches defined unacceptable levels (U_R) (Figure 2). The unacceptable level may be decided from an ultimate strength or serviceability point of view. When such a criteria is used, yielding in some part of the structure

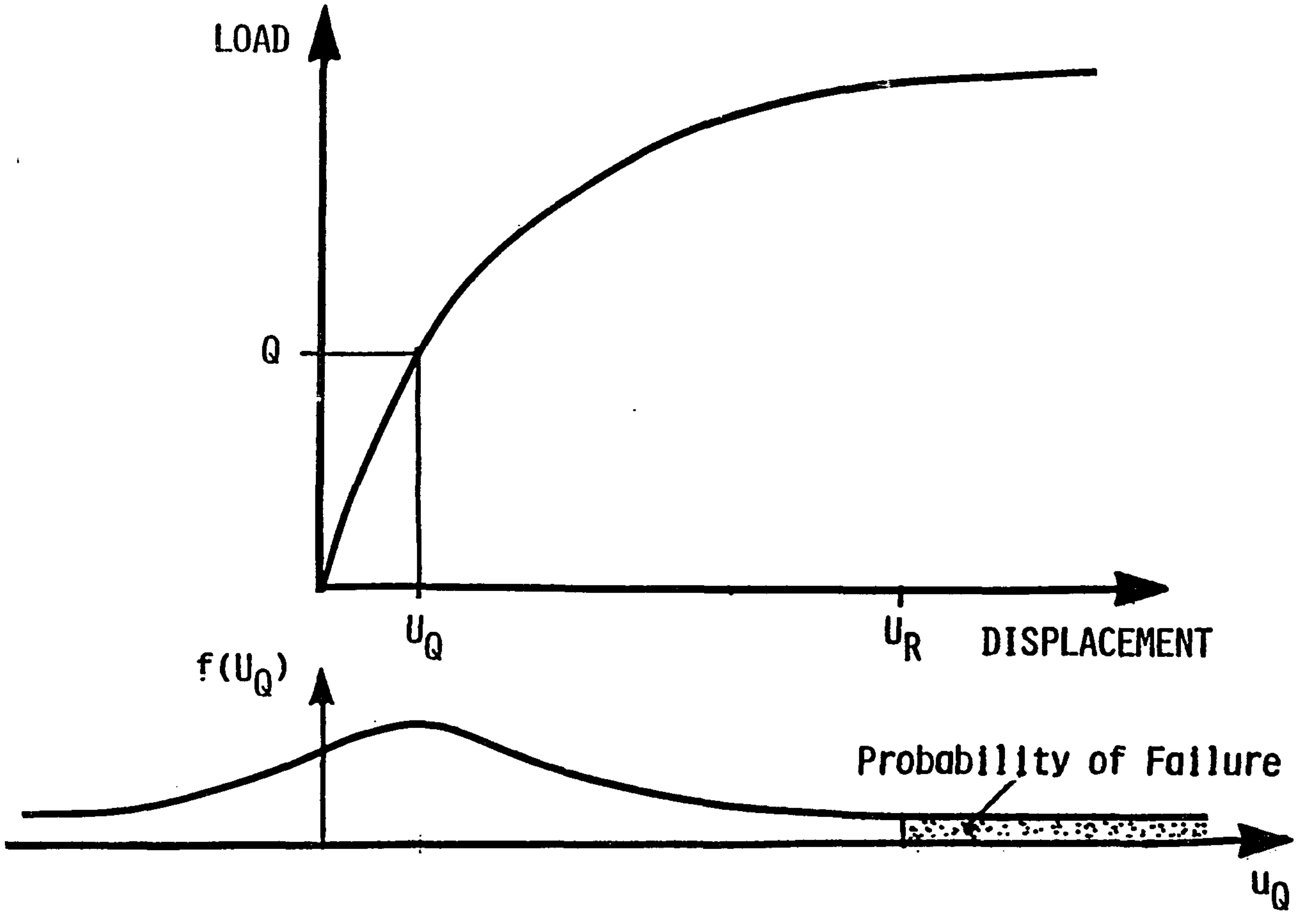

Figure 2. Structural response and probability of failure

does not imply that the overall structure has failed. For the true representation of the structural model, the nonlinear behavior of the material beyond elastic limits is often required. Therefore, a nonlinear finite element analysis is necessary to represent the structural model.

To summarize, the statistics of the basic variables are assumed to be known. The structural behavior is analyzed using a nonlinear finite element analysis. The structure is considered to have failed if the global deflection exceeds certain levels. The problem is to determine the probability of failure.

1.3. Objective and Scope

A nonlinear finite element analysis requires an extensive computational effort. If a simulation procedure is set up to estimate the probability of failure, the finite element analysis has to be conducted many times. Such a procedure is not economical. The objective of this work is to develop a reliability method, such that the finite element analysis is carried out a reasonable number of times. This objective is achieved in the following chapters.

In Chapter 2, the structural reliability theory and methods are reviewed. These methods are examined keeping in mind that the structural model is not described by a simple expression. Finally, the outline of the proposed technique is presented.

In Chapter 3, a method called gradient analysis is developed to study the influence of the basic parameters on displacements, that is, sensitivities. The gradient analysis is performed by direct differentiation of the matrix equilibrium equation and gradient computations are done parallel to the structural analysis. The gradient analysis scheme is presented in an algorithm.

In Chapter 4, the gradient analysis is applied to planar trusses. The material behavior is represented by a modified Ramberg-Osgood equation. Examples are worked to test the validity of the gradient analysis algorithm.

In Chapter 5, the gradient and finite element analyses are used to formulate an approximate expression for the failure function. This approximate expression is used in the Monte Carlo procedure to evaluate the probability of failure. This technique is identified as the "Response Failure Surface Method".

In Chapter 6, the above technique is applied to the plane truss examples of Chapter 4. The areas of the cross section, Young's modulus, yield stress and the shape of the stress-strain curve are considered as basic parameters. The probability of failure is determined by the Response Failure Surface Method. The probability of failure is also determined by Advanced First Order Second Moment (AFOSM) method with gradients obtained by the methods of Chapter 3. The results of the probability of failure from AFOSM method, Response Failure Surface Method, are compared to the exact limit state method. In exact limit state method, the actual failure function is used in the Monte Carlo procedure to evaluate the probability of failure.

In Chapter 7, the main conclusions from the above chapters are summarized. Future research areas are suggested.

2. REVIEW OF STRUCTURAL RELIABILITY METHODS

2.1. Introduction

Several structural reliability methods have been developed in the last decade. The methods that are related to the present study are reviewed here. In the beginning of this chapter, the basic elements of structural reliability are explained. A method called "Response Failure Surface Method". is proposed in the last section and the outline of this method is explained.

2.2. Elements of Structural Reliability

2.2.1. Random variables

A quantity which exhibits uncertainty and variation in its value is known as a random quantity (3). In a structural problem, the design variables (dimensions and strength parameters) and load quantities exhibit variability and are, thus, identified as random quantities. Usually, a random quantity is called a "random variable" if its value and uncertainty does not vary in time. If the random quantity does vary with time, it is known as "random process" or "stochastic process". An example of the random process is the live load on the structure. In this study, the structural parameters are considered to be independent of time. All the parameters are considered as random variables and represented by a vector {x}.

To describe the randomness of a variable, a statistical approach is taken. A sample of data is collected and subjected to statistical analysis. The randomness of a variable is described by its mean, variance, correlation with other variables, and probability density function. For example, the yield strength of steel can be statistically characterized as a lognormally distributed random variable (4). In this study, complete statistical information on random variables is assumed to be available.

2.2.2. Limit state function

The limit state is defined by:

> "A structure or part of a structure is considered unfit for use when it exceeds a particular state, called a limit state, beyond which it infringes one of the criteria governing its performance or use (3)."

There are two types of limit states: an ultimate limit state, which corresponds to the collapse of the structure; and a serviceability limit state which corresponds to the functional use of the structure. A typical list of the above limit states can be found in Reference 3.

The limit state is a function of the basic variables such as strength and loading parameters and can be expressed as (4, 9, 22)

$$G = G\ (\ \{x\}\ ) \tag{2.1}$$

where {x} is a one by N vector of the random variables. One simple example of the limit state for two variables is as follows. Consider the displacement in a axially stretched bar as U_Q and the displacement at yield of the bar as U_R. Let U_Q and U_R be the random variables. The failure function or the limit state can be expressed as

$$G = G\ (U_R,\ U_Q) = U_R - U_Q \tag{2.2}$$

The bar is considered to have reached a limiting state if G is less than zero, i.e., the displacement in the bar has reached an unacceptable level. In the above limit state, the term U_R represents the structural resistance (R) and U_Q represents the load effect (Q). Therefore, in general, a limit state is expressed as

$$G = R - Q \tag{2.3}$$

In a structural problem, the limit state is frequently in the form of Equation 2.3. For a general case, G need not be restricted to only two variables; R and Q can be functions of many variables (x). For example, in Equation 2.2, the term U_Q could be related to load, cross-sectional area, elastic modulus, and length of the bar.

2.2.3. Probability of failure

The limit state function or the failure function is expressed in terms of random variables as in Equation 2.1. Since the variables, {x}, are random, the value of the limit state (G) is also expected to be random. Therefore, there is a probability that the limit state will be attained, i.e., G will be less than zero. This probability is defined as the probability of failure and written as (3, 4, 9)

$$p_f = P\ (G<0) = \int_{-\infty}^{0} f(G)\ dG \qquad (2.4)$$

where f(G) is the probability density function of G{x}, as illustrated in Figure 3. Since the limit state function G is a function of {x}, Equation 2.4 can also be expressed as (3, 4, 9)

$$p_f = \int \cdots\cdots\cdots \int_{D(G<0)} f_x(x_1,\ x_2, \ldots x_N) \qquad dx_1 \ldots dx_N \qquad (2.5)$$

in which f_x is the joint probability density function for x_1, $x_2, \ldots x_N$. In Equation 2.5, the integration is performed over the failure domain, i.e., D(G<0).

To understand the application of the above concept, consider a limit state with two variables, R and Q (Equation 2.3). Assume that the values of R and Q are greater than zero. The failure domain, where G is less than zero, is shown in Figure 4. The probability of failure is the volume under

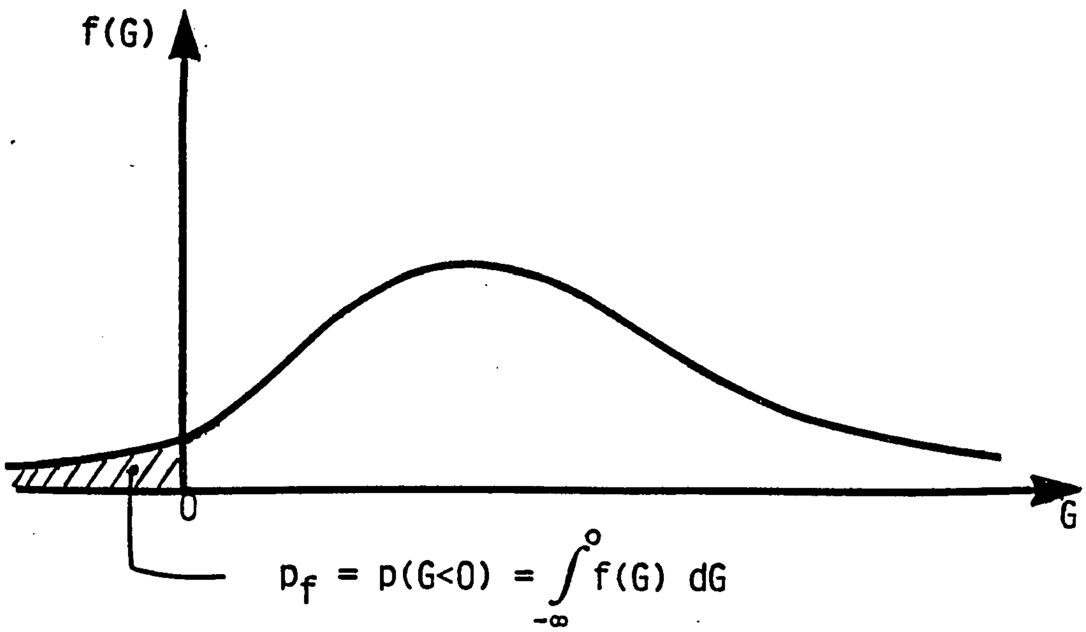

Figure 3. Probability density of a failure function

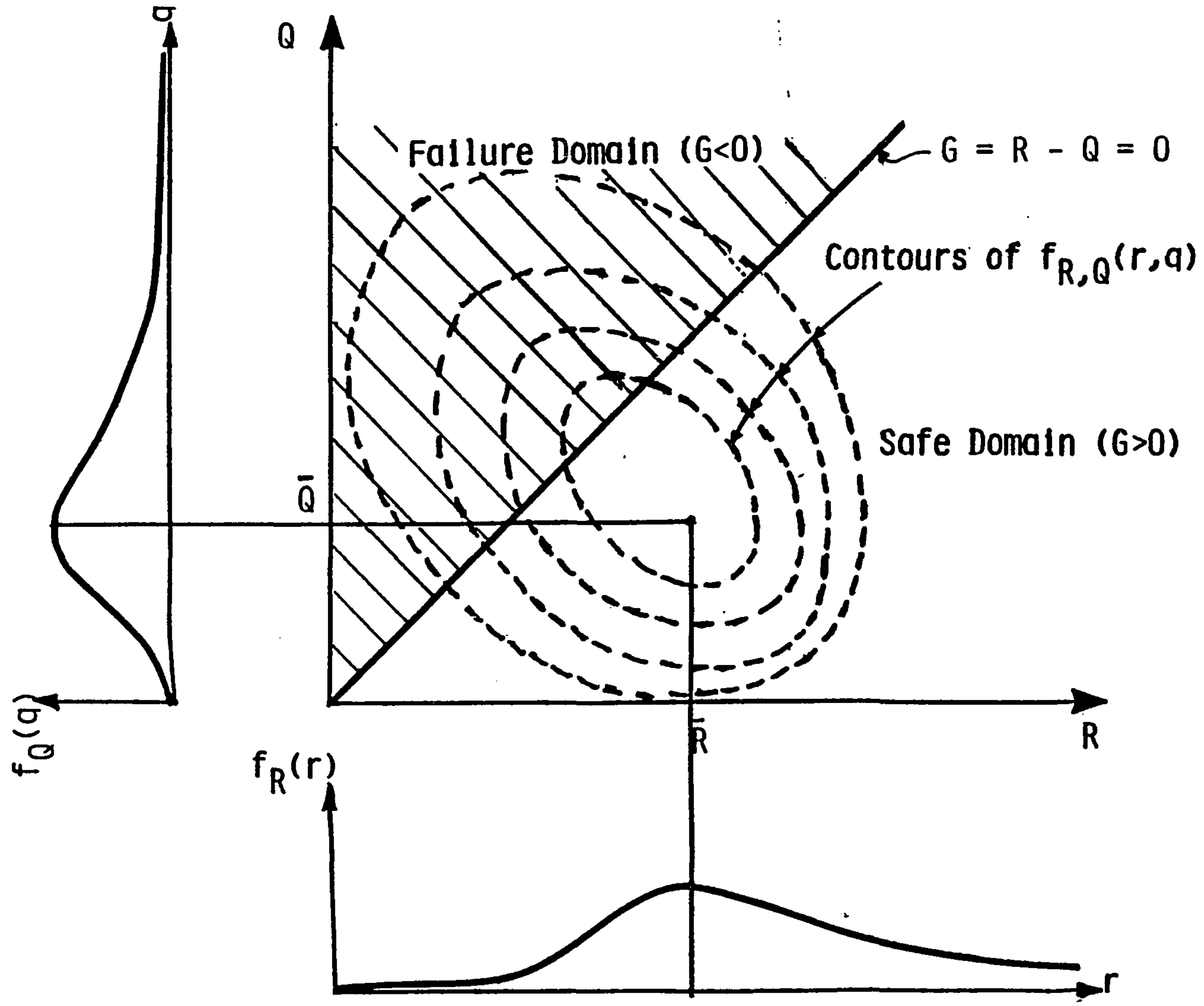

Figure 4. Integration of $f_{R,Q}(r,q)$ in the failure domain to obtain p_f

the joint probability density function of R and Q in the failure region. If R and Q are considered as independent variables, p_f can be written as (4, 9)

$$p_f = P(R<Q) = \iint_{D(R<Q)} f_R(r)\ f_Q(q)\ dr\ dq \qquad (2.6)$$

The above equation can also be written as

$$p_f = \int_0^\infty f_Q(q) \left[\int_0^q f_R(r)\ dr \right] dq$$

$$= \int_0^\infty F_R(q)\ f_Q(q)\ dq \qquad (2.7)$$

in which $F_R(q)$ is the cumulative probability distribution function of the random variable R.

Suppose R and Q have normal probability density functions, and let μ_R and σ_R be the mean and standard deviation, respectively, for R and similarly for Q. Then, the integral of Equation 2.7 is given by

$$p_f = \Phi\ (-\beta) \qquad (2.8)$$

in which

$$\beta = \frac{\mu_R - \mu_Q}{\sqrt{\sigma_R^{\ 2} - \sigma_Q^{\ 2}}} \qquad (2.9)$$

where Φ (.) is the cumulative standard normal distribution. The quantity β is referred to as the "reliability index". If

R and Q both have lognormal distributions, then the failure probability is approximated by Equation 2.8, in which

$$\beta = \frac{\ln (\mu_R / \mu_Q)}{\sqrt{V_R^2 + V_Q^2}} \qquad (2.10)$$

where V_R and V_Q are the coefficients of variation of R and Q, respectively.

For the cases when G is a nonlinear function of several variables, deriving an expression similar to Equations 2.8, 2.9 and 2.10 for the failure probability is extremely difficult, if not analytically impossible. In the literature, various reliability methods have been developed to solve this problem, i.e., to evaluate the probability of failure. The problem gets more complicated if G is not in the form of an explicit expression. In the present study, the overall structural reliability of the ultimate limit states is of interest. The overall behavior is to be predicted by a finite element technique (Chapter 1). The limitation of the elastic structural theory for the evaluation of the ultimate limit state is well-recognized. Nonlinear material behavior must be considered in the finite element analysis. Thus, G is evaluated by a nonlinear finite element technique on a point-by-point basis.

2.3. Review of Structural Reliability Methods

In literature, several methods have been developed to evaluate the integral of Equation 2.5, i.e., p_f. These methods are reviewed below considering the practicality and suitability of each method when the limit state is evaluated by a nonlinear finite element analysis.

2.3.1. Monte Carlo method

This method is a statistical approach for the evaluation of the integral of Equation 2.5. In this method, a set of random values are generated for all the random variables (17, 21). These values are substituted into Equation 2.1 to evaluate G. If the value of G is less than zero the structure is considered to have failed. This simulation process is repeated many times. The probability of failure is the ratio of the number of times G is less than zero to the total number of simulations. This procedure is explained in detail in Chapter 5.

From a theoretical point of view, the estimate of the probability of failure will approach the exact value when the number of simulations tends to infinity. A large number of simulations is required to predict low probabilities with sufficient accuracy. If applied to this study, every simulation is one nonlinear finite element analysis. Therefore, for a large number of experiments, the computational cost will be very high.

In order to reduce the number of simulations, methods such as variance reduction techniques have been proposed (18, 21). In these techniques an explicit expression for the limit state G is required. The application of these techniques when G is evaluated by a numerical procedure is not evident. Also, these techniques are highly problem dependent and there is no guarantee of the success of the method (21).

2.3.2. Second moment methods

In the second moment methods, the uncertainty of each random variable is characterized by its mean and its standard deviation. The limit state function G(x) is linearized at the mean of {x} with the first two terms of a Taylor series expansion. The first two statistical moments of G are calculated. The probability distribution of G is approximated by a normal distribution to evaluate the probability of failure (22). This method is known as the Mean Value First Order Second Moment (MVFOSM) method. Such a procedure is used in Reference 20 to evaluate the mean and standard deviation of the stresses in a flange joint. A finite element program is used to determine the stresses. The gradients that are needed to calculate the variance of the stresses are determined by a finite differencing method. The criticism against the MVFOSM method is that the approximation of G is done at the mean values of the random variables. Since G(x) is nonlinear in a structural problem, significant errors could result in the calculation of the probability of failure. Another source of error is in the approximation of the probability distribution of the limit state by a Gaussian distribution. Finally, different probabilities of failure are obtained from the MVFOSM with different, but equivalent, formulations of the limit state (15). For example, for the limit state of Equation 2.3 the p_f is given by Equations 2.8 and 2.9. An alternate formulation of Equation 2.3 can be written as

$$G = \frac{R}{Q} - 1 \tag{2.11}$$

For such a limit state, the β is different than Equation 2.9 and is given by

$$\beta = \frac{\mu_R - \mu_Q}{\sqrt{\sigma_R^2 + \sigma_Q^2(\mu_R/\mu_Q)^2}} \tag{2.12}$$

As an improvement over the MVFOSM method, an invariant second moment method was developed by Lind and Hosofer (refer to 4, 9, 22). This method is called Advanced First Order Second Moment (AFOSM) method. The basic principle involved in the AFOSM method is that the limit state function G is linearized at a point on the failure surface (G equal to zero). The distance from the mean values of the variables to the point of linearization is related to β (refer to Chapter 5). Then, the probability of failure is determined by Equation 2.8. This method is explained in detail in Chapter 5.

In the AFOSM method, the point of linearization is determined by an iterative procedure. Therefore, many number of functional evaluations of G may be needed. In order to locate the linearization point, the gradients of the limit state with respect to the basic variables, i.e., dG/dx, are required. As explained before, a closed form expression for G is not available and a nonlinear finite element analysis must be used in the evaluation of G and its gradients. The AFOSM method can give an exact p_f only for the case of a linear G and multinormal joint probability distributions of the basic variables. In both the MVFOSM and AFOSM methods, the p_f can at best be only bounded if the failure is defined by more than one failure function (more than one G). (Refer to Section 5.3.3.)

2.3.3. Response surface method

As an alternate to the large number of finite element evaluations required above, the finite element analysis can be performed a limited number of times and an analytical function fit through these limited results to approximate the limit state. This approximate function is called a response surface. Now, the probability of failure can be evaluated by using Monte Carlo procedure (36) and/or AFOSM method (14, 37). In these probability methods, the limit state is represented by the response surface because the evaluation of G with the response surface is computationally much more inexpensive than a complete nonlinear FE analysis.

This approach was taken by Wong (36) to study the dynamic soil structure interaction problem. Two level factorial design is used in the development of the response surface, i.e., each variable takes on two values in addition to the mean. These two levels correspond to plus or minus one standard deviation from the mean. A total of 2^N finite element analyses are done based on all possible combinations of these perturbed values of the variables. A high degree polynomial is fit through the finite element results to represent the approximate G function in all regions.

The above procedure approximates the G function only in the vicinity of the mean values of G. Usually, the boundary between the safe and unsafe region is far from the mean value of G. Therefore, the approximate surface may not match the exact failure surface for G in the regions of high failure probability density. In general, the G function in a structural problem is strictly monotonic with respect to the basic variables. When such a function is represented by a higher degree polynomial, it may no longer be strictly monotonic. This may result in inappropriate pockets of unsafe regions. Finally, as the number of variables (N) increases, the number of finite element analysis (2^N) will increase drastically.

2.3.4. Improved 2N+1 method

The improved 2N+1 method is an approach developed by Gorman and Moses (13) that uses the first four statistical moments of the basic variables to estimate the first four statistical moments of the G function. First, a finite element analysis is conducted at the mean. Other finite element analyses are performed by changing one variable at a time. The total number of finite element analyses is equal to 2N+1. From these 2N+1 analyses, an approximate expression for the limit state in product form is developed. This expression can be viewed as a special case of the response surface. This expression is used in finding the first four statistical moments of G. These moments can be associated with the Pearson distribution (15, 17) to enable probability statements to be made using Equation 2.4.

The results from this method were compared with Monte Carlo method (13). An excellent agreement was found between the mean values of G. The second moments of G had reasonable agreement. Third and fourth moments did not seem to match well with the Monte Carlo results. Even if the four moments were exact, the validity of the Pearson distribution to represent the probability density function of G may not be appropriate. In Reference 15, the probability of failure of some structural systems is estimated by Monte Carlo, the improved 2N+1 method and AFOSM method. The authors of

Reference 15 found that the probability of failure estimated by the improved 2N+1 method did not give satisfactory results when compared with the Monte Carlo method.

2.3.5. Unzipping methods

Another approach to system reliability of trusses and frame systems was proposed by Moses and Stahl (refer to 24, 26). A linearized expression for the system resistance is obtained by an incremental load method. The structure is analyzed under a unit load to find the critical component, i.e., the component which will first reach its mean resistance. The load required to reach the mean component failure is expressed in terms of the element resistance. The critical component is then replaced by its mean post-failure strength (yield strength if elastic-plastic, zero if brittle) and the system is reanalyzed with a unit load to find the next component failure. The analysis is repeated by removing a failed component at each step (unzipping) and continuing until the system collapses. The outcome yields a resistance expression in terms of the unzipped element resistances. This expression can be combined with the load variable to get an expression for G. Probability of failure results can be obtained by Monte Carlo simulation using this G expression. The simple form of the G expression permits a large number of simulations as compared to a relatively expensive finite element evaluation (27).

The major drawback of this method is that it will yield only one failure mode, as determined by mean component resistances. There appears to be no criteria for establishing the significance of the derived mode. A heuristic technique such as trial Monte Carlo is suggested (25).

Recently, Melchers and Tang (23) have proposed a method called truncated enumeration method which has many features of the incremental load method. In the truncated enumeration method, all the dominant failure modes are searched iteratively by constructing an event-tree. Such an approach was used by Guenard (16) in the estimation of system reliability of offshore structures.

The unzipping methods are developed only for the elastic-plastic and brittle systems. The only random variables are the element resistances. There is no way to incorporate any other variables such as the elastic properties, geometry, etc. The method seems to be suited only for truss and frame systems. An application of this method to continuous systems is not evident. The unzipping methods are specialized for the case where the ultimate strength is the limit state. Displacements are not a criteria for failure. At times, unzipping several members may introduce large displacements and invalidate the linearized structural analysis (25).

2.3.6. Other methods

Numerical integration formulas are developed by Gorman (12) to evaluate the first four statistical moments of the structural resistance. Formulas are developed for the special case of normal and lognormal distributed random variables. These integration formulas are used in the examples in Reference 12 to evaluate the statistical moments of the structural resistance. The formulas did not give consistent and comparable results for the third and fourth statistical moments when compared to Monte Carlo results. As is the case with the improved 2N+1 method, exact structural resistance moments do not ensure an accurate probability of failure.

A procedure has been developed by Vanmarke (35) for obtaining the first and second statistical moments for the deflection of the structural members whose properties vary randomly along their axis. Finite elements subdivide the region, and the mean characteristics of each element are assumed to be equal to the local average over the element length. The covariance matrix of these element averages is obtained by simple algebraic operations on the variance function. The mean and covariance matrix of the elemental characteristics are then related to first two moments of the structural deflection and stresses by MVFOSM method. The significant contribution of this work (35) is the evaluation of the means and covariance matrix of the properties of the individual finite elements.

2.4. Outline of the Proposed Method

Before describing the proposed method, the reliability methods that were discussed will be summarized. In order to avoid the expensive Monte Carlo analysis, second moment methods were developed. These methods were developed for simple analytical forms of the limit state function. These methods are not readily applicable unless there is a method to find the gradients of the limit state with respect to basic variables. Therefore, methods such as improved 2N+1 method, response surface method, unzipping methods, and numerical integration method were developed, where the gradient computations are not required. These methods are suitable for situations in which finite elements are used as the analysis tool for the evaluation of G function.

In all the above methods (except Monte Carlo), the idea of representing the limit state in a simple form is used. For example, in MVFOSM method, the truncated Taylor's series is used as an approximation to the actual limit state function (G(x)). To do so, the value of G and its gradients, dG/dx, are evaluated at the mean values of the random variables. In Figure 5, the location for the evaluation of G, i.e., the values of the random variables for a finite element analysis,

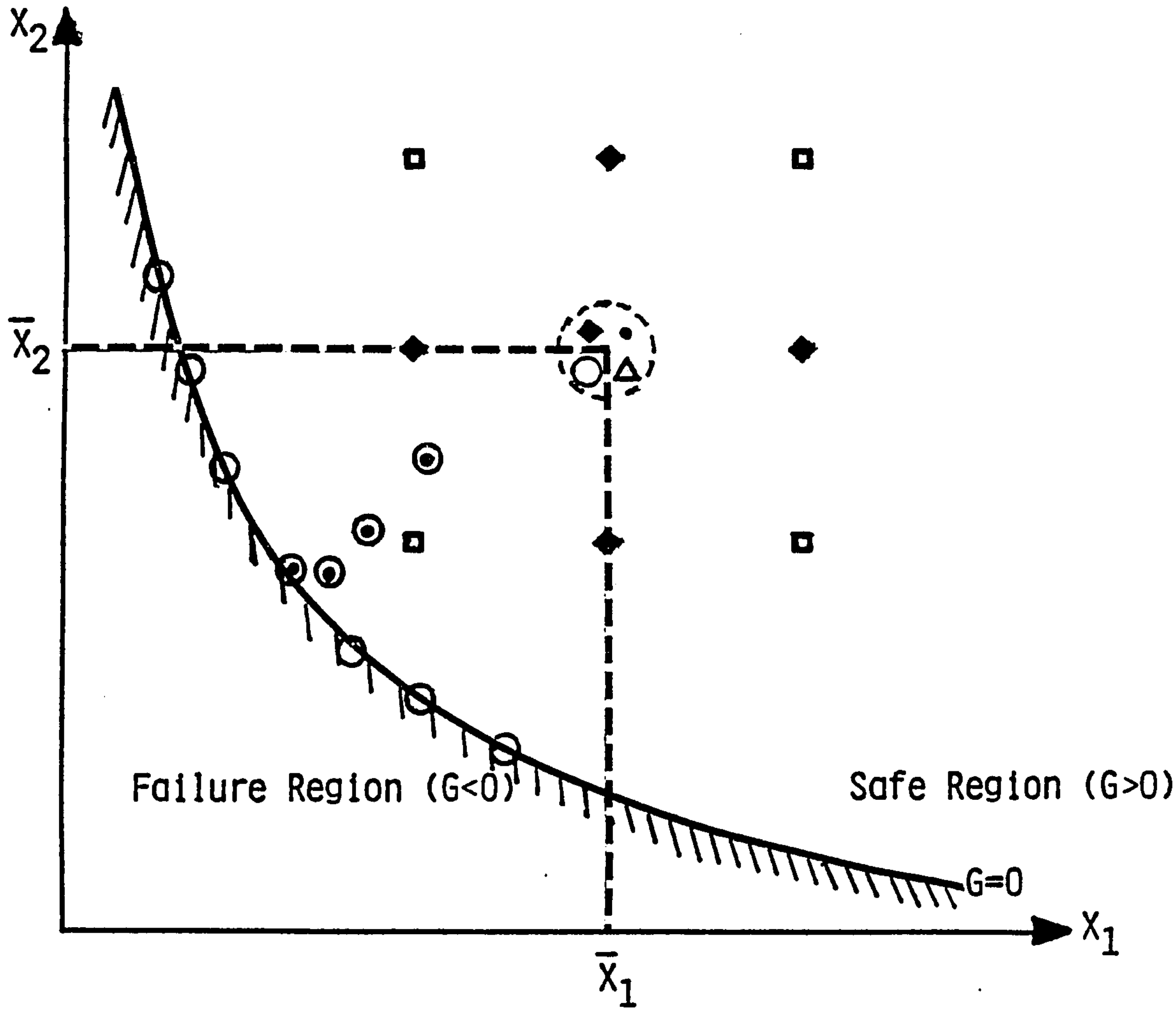

△ MVFOSM method: FE and Gradient Analysis

● AFOSM method: FE and Gradient Analysis

◆ Response Surface Method by Wong: FE Analysis

□ Improved 2N+1 method: FE Analysis

○ Proposed "Response Failure Surface Method": FE and Gradient Analysis

Figure 5. Finite element analysis in different reliability methods

are shown for the two variable case. Among all methods shown, AFOSM method has a unique feature. In AFOSM method, the approximation to the failure surface (G(x) = 0) is sought and not an approximation to the failure function (G(x)). Therefore, the linearization of the limit state is done at a point on the failure surface, G(x) = 0. The gradients are used to locate such a point on the failure surface and to obtain an expression for linearized surface. This approach is more meaningful when the probability of failure is of interest and not the statistical moments of G function.

Such an idea is used in the present study. An approximation to the failure surface (G(x) = 0) is needed. Therefore, the evaluation of G and its gradients are done at points on the failure surface (Figure 5). The values of G and dG/dx from each analysis are used for locating the next point for the analysis. Finally, the values of G and dG/dx from all the analyses are used in forming the approximate failure surface. This approximate expression is called the "Response Failure Surface". The probability of failure is estimated by Monte Carlo in which the response failure surface is used to predict the structural failure or success. This approach is shown in Figure 6. This method is referred to as the "Response Failure Surface Method".

The results of the p_f from the above method are compared with the results from the exact limit state method and the

AFOSM method (Figure 6). In exact limit state method, the exact failure function, G, is used in Monte Carlo analysis. The outline of the above task is depicted in Figure 6.

Chapters 3 and 4 will focus on the development of the gradient analysis and its illustration. In Chapter 5, the response failure surface method and AFOSM method will be explained. Examples follow in Chapter 6.

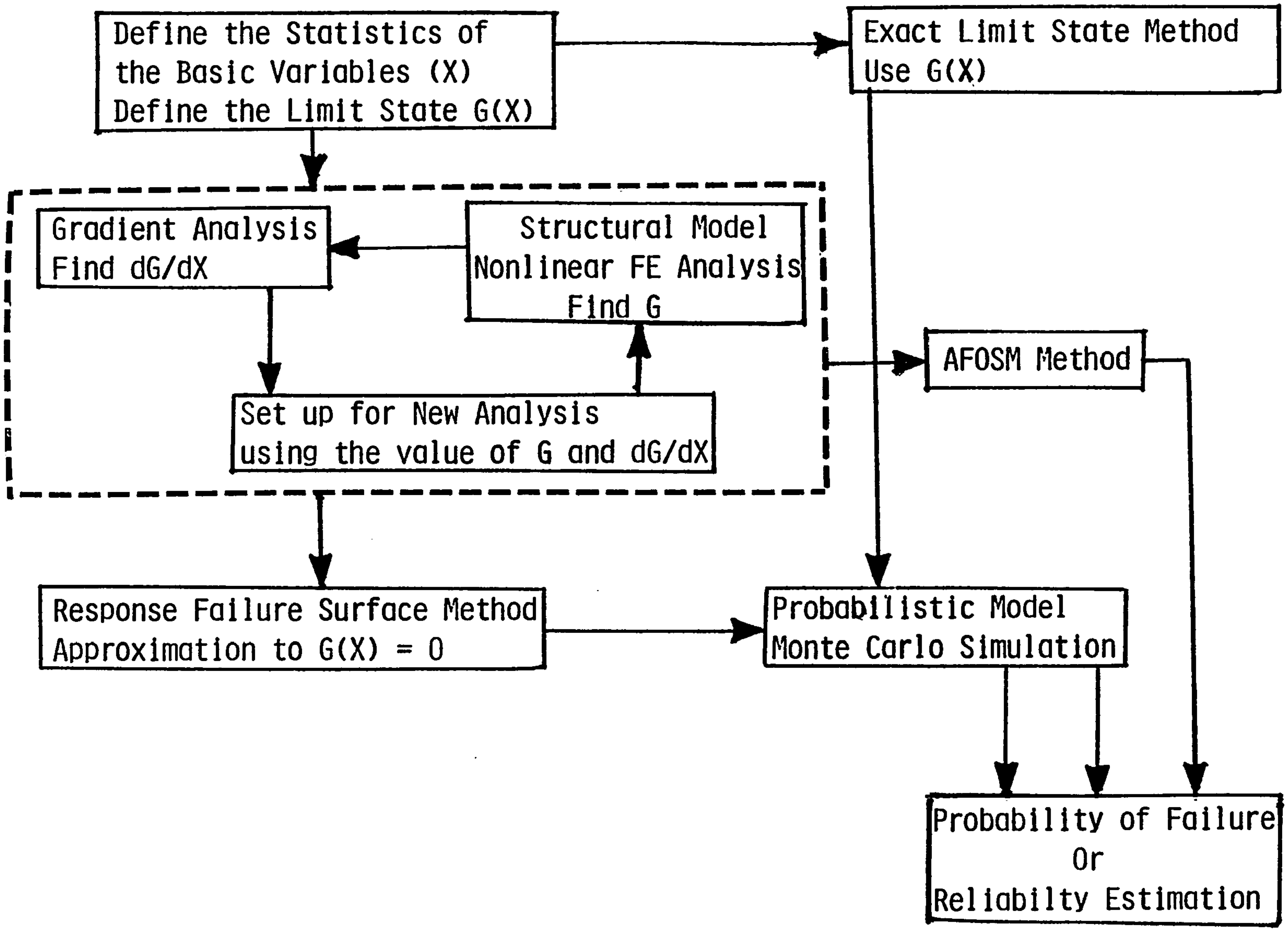

Figure 6. Outline of the present work

3. GRADIENT ANALYSIS OF NONLINEAR STRUCTURAL SYSTEMS

3.1. Introduction

The finite element technique has been used as a structural analysis tool in the field of structural optimization (34). Many of the optimization methods require gradients of the cost function and the constraint functions with respect to design variables. Typically, a constraint function is a limitation on the deflections and/or stresses. The gradients of deflections and stresses are necessary to find the gradients of the constraint function. In a reliability study, the constraint function is a limit state function. The gradient information of the limit state is also necessary in reliability methods such as AFOSM method. The derivatives of the deflection and stresses can be determined approximately by changing the design variable and performing a new finite element analysis, i.e., a finite difference approximation to first derivative. If such a procedure is used for the N variable case, there will be N more new finite element analyses. This approach is found to be costly for complex structures and, also, the gradients are not exact (34). The error between the calculated gradients and the exact gradient is not known. For this reason, methods have been developed to make the gradient computation an integral part of the finite element analysis and obtain exact gradients. In the literature, this approach is often referred to as "Sensitivity Analysis" (2, 33).

The gradient analysis is carried out by differentiating the equilibrium equation with respect to the basic variables (in structural optimization, basic variables are called design variables) (2, 19). This scheme has been developed and demonstrated with examples for the case of linear systems (2, 10, 19). In this study, the nonlinear behavior of the structure, due to material nonlinearity, is considered. Therefore, a nonlinear finite element technique will be used for the structural analysis. The present task is to develop a gradient analysis technique in conjunction with the nonlinear finite element analysis. This will be accomplished by considering each iteration in a nonlinear solution to be a linear analysis.

3.2. Gradient of Limit State Functions

A general limit state function G is defined by

$$G = G\left(\{x\},\{U\},\{\sigma\}\right) \tag{3.1}$$

where $\{x\}$ is the vector of basic (or design) variables, $\{U\}$ is the vector of displacements and $\{\sigma\}$ is the vector of stresses. In general, the basic variables are the geometric and material properties of the structural elements. One example of a limit state is the displacement constraint (refer to Chapter 2):

$$G_j = 1 - \frac{U_j}{U_{Rj}} \qquad j = 1,\text{NDOF} \qquad (3.2)$$

where U_j is the j^{th} nodal displacement of the structure and U_{Rj} is some limiting displacement. There could be many such constraints on displacements and stresses. The gradients of G with respect to a basic variable x_k are obtained by differentiating Equation 3.1 as

$$\frac{dG}{dx_k} = \frac{\partial G}{\partial x_k} + \left\{\frac{\partial G}{\partial U}\right\}^T \left\{\frac{dU}{dx_k}\right\} + \left\{\frac{\partial G}{\partial \sigma}\right\}^T \left\{\frac{d\sigma}{dx_k}\right\} \qquad (3.3)$$

Note that $\{\partial G/\partial U\}$ and $\{dU/dx_k\}$ have the same dimension as $\{U\}$, whereas $\{\partial G/\partial \sigma\}$ and $\{d\sigma/dx_k\}$ have the same dimension as $\{\sigma\}$. Since G is usually represented in a form such as Equation 3.2, $\partial G/\partial x_k$, $\{\partial G/\partial U\}$ and $\{\partial G/\partial \sigma\}$ can be obtained by an explicit differentiation. In a complicated structural problem, it is not possible to have closed form expressions for $\{U\}$ and $\{\sigma\}$ in terms of the basic variables $\{x\}$ and, hence, explicit expressions for $\{dU/dx_k\}$ and $\{d\sigma/dx_k\}$. The primary objective of this chapter is to evaluate $\{dU/dx_k\}$ and $\{d\sigma/dx_k\}$. These gradients are referred to as the gradients of the structural response with respect to the basic variables.

3.3. Gradient Analysis in Linear Elastic Analysis

The linear structural behavior is predicted in the finite element analysis by the evaluation of the matrix equation (5)

$$[K]\{U\} = \{F\} \tag{3.4}$$

where the global stiffness matrix, [K], is the superposition of elemental stiffness matrices, [k], given schematically by

$$[K] = \sum_{i=1}^{NE} [k_i] \tag{3.5}$$

{F} is the vector of applied loads and {U} is the vector of nodal displacements. Differentiating the equilibrium Equation 3.4, with respect to a basic variable x_k will yield (2, 10, 19, 33)

$$[K]\left\{\frac{dU}{dx_k}\right\} + \left[\frac{dK}{dx_k}\right]\{U\} = \left\{\frac{dF}{dx_k}\right\}$$

rearranging

$$[K]\left\{\frac{dU}{dx_k}\right\} = \left\{\frac{dF}{dx_k}\right\} - \left[\frac{dK}{dx_k}\right]\{U\} \tag{3.6}$$

This set of equations are solved for $\{dU/dx_k\}$ by making use of the available factored global stiffness matrix from the analysis phase (solution of Equation 3.4). On the right hand side, matrix $[dK/dx_k]$ is obtained by differentiating the elemental stiffness matrices with respect to the basic variable x_k under consideration and assembling the differentiated matrices. This is represented by differentiating (3.5) as

$$\left[\frac{dK}{dx_k}\right] = \sum_{i=1}^{NE} \left[\frac{dk_i}{dx_k}\right] \tag{3.7}$$

In Equation 3.6, the vector $\{dF/dx_k\}$ is equal to zero unless the applied set of basic forces are also considered as the basic variables or functions of the basic variables. To obtain matrix [dU/dx], Equation 3.6 has to be solved for each basic variable, i.e., for all k.

The stress component $\{\sigma\}$ in an element is directly related to its nodal displacement {U} as (5)

$$\{\sigma\} = [E]\,[B]\,\{u\} \tag{3.8}$$

where [E] is the matrix of material properties, [B],which is the strain-displacement matrix, is a function of the nodal coordinates and {u} is the element nodal displacements. The gradients of stress components can be evaluated by differentiating Equation 3.8 with respect to basic variables x_k as

$$\left\{\frac{d\sigma}{dx_k}\right\} = \left[\frac{dE}{dx_k}\right] [B]\,\{u\} + [E][B]\left\{\frac{du}{dx_k}\right\} \tag{3.9}$$

where $\{du/dx_k\}$ is the elemental subset of $\{dU/dx_k\}$. The term $[dB/dx_k]$ is zero unless the nodal coordinates are also the basic variables. Thus, the stress gradients are related to the displacement gradients, which are obtained from Equation 3.6.

3.4. Nonlinear Elastic Cases

3.4.1. Nonlinear finite element analysis

The Newton-Raphson iteration method is used for the nonlinear analysis (5). The approach is the tangent stiffness technique where, in a given load increment, the iteration method is applied so that the element nodal displacements are successively corrected until the joint equilibrium is satisfied. These displacement corrections are computed using element tangent stiffness matrices, which are successively updated to reflect the current state of the total displacement, total stress, and the material properties. The equilibrium equation in the j^{th} load increment and the i^{th} iteration is given by (Figure 7) (5)

$$\left[K_T(U_j^{i-1},x)\right]_j^{i-1}\left\{\Delta U\right\}_j^{i}=\left\{F(x)\right\}_j-\left\{P(\sigma_j^{i-1},x)\right\}_j^{i-1} \qquad (3.10)$$

where $\left[K_T(U_j^{i-1},x)\right]_j^{i-1}$ is the global tangent stiffness matrix formulated as a function of the current displacements $\{U\}_j^{i-1}$ and the basic variables $\{x\}$. The vector $\{U\}_j^{i}$ is the current displacement increment for the i^{th} iteration. The current total internal force $\{P(\sigma_j^{i-1},x)\}_j^{i-1}$ is formulated as a function of the current stress $\{\sigma\}_j^{i-1}$ and $\{x\}$,

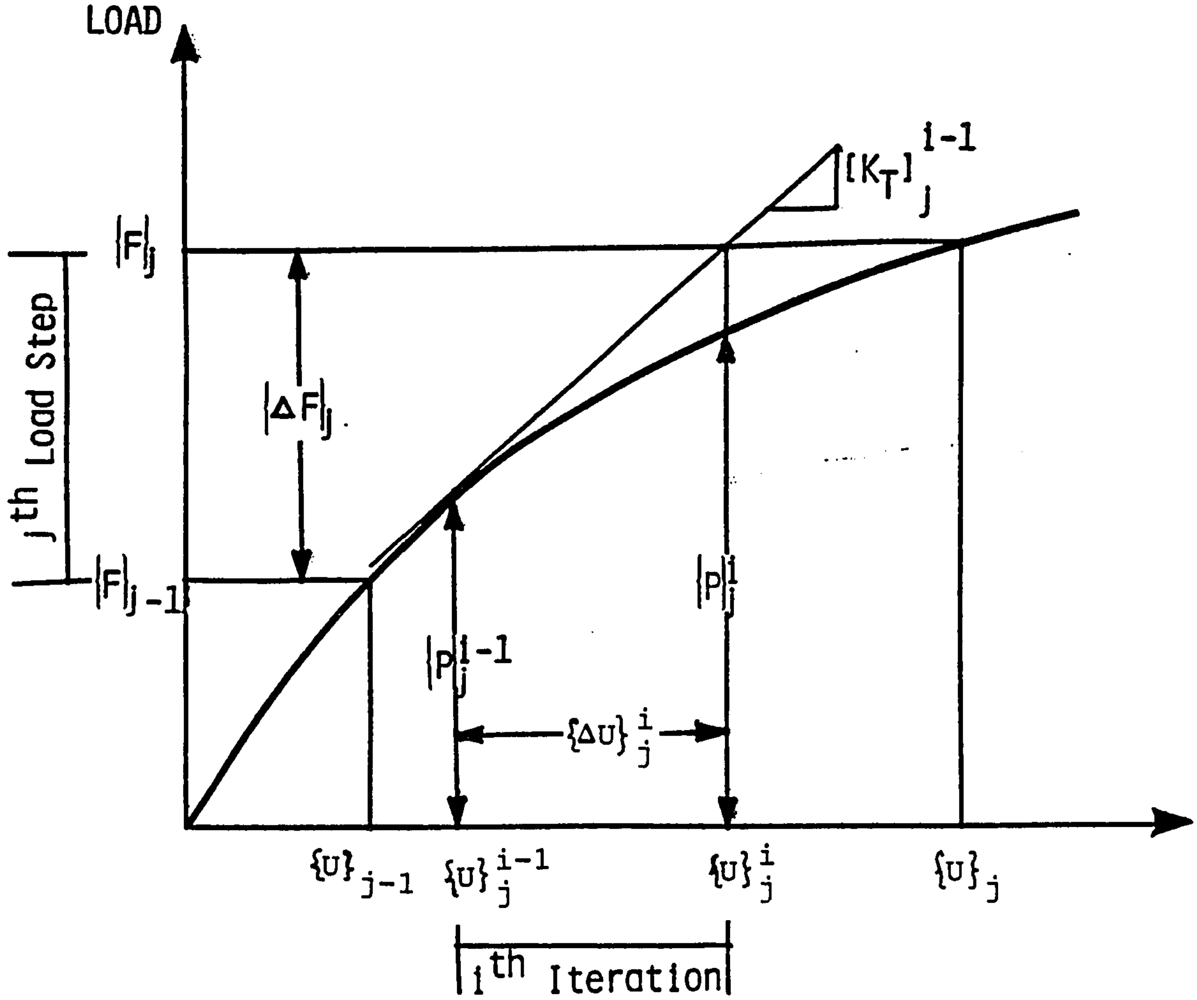

Figure 7. Newton-Raphson iteration for nonlinear analysis

$$\{P\}_j^{i-1} = \sum_{1}^{NE} \int_V [B]^T \{\sigma\}_j^{i-1} \, dV(x) \tag{3.11}$$

Equation 3.11 represents the volume integral of all the elements and the subsequent assembly.

The right hand side vector of Equation 3.10 is the current unbalanced force. The Newton-Raphson method, thus, attempts to find an equilibrium solution for an increment of external load, $\{\Delta F\}$, by forcing the unbalanced force to be as close to zero as possible through a series of iterations. The increment of displacement $\{\Delta U\}$ is added to the previous displacement to form a new total displacement

$$\{U\}_j^i = \{U\}_j^{i-1} + \{\Delta U\}_j^i \tag{3.12}$$

The increment in the stress component in an element is directly related to the incremental displacements.

$$\{\Delta\sigma\}_j^i = \left[E_T(u_j^{i-1}, x)\right]_j^{i-1} [B]\{\Delta u\}_j^i \tag{3.13}$$

where $[E_T(u_j^{i-1}, x)]_j^{i-1}$ is the matrix of material properties, which is a function of both displacements and the basic variables, and $[B]$ is a function of nodal coordinates. The term $\{\Delta u\}_j^i$ is the incremental displacement of the element which is a subset of $\{\Delta U\}_j^i$. The stress increment is added to the previous stresses to form the new total stresses

$$\{\sigma\}_j^i = \{\sigma\}_j^{i-1} + \{\Delta\sigma\}_j^i \tag{3.14}$$

The iterative solution is obtained for all the load steps and the final displacement {U} and stresses {σ} are obtained by summing the results from all the load steps.

3.4.2. Gradient analysis

The nonlinear gradient analysis can also be accomplished by successive linear approximations. The concept follows the differentiation of the equilibrium Equation 3.10 in each iteration for all the load steps. The differentiation of Equation 3.10, with respect to the basic variable x_k, with other variables held constant can be written as

$$\left[K_T(U_j^{i-1},x)\right]_j^{i-1}\left\{\frac{d\ \Delta U}{dx_k}\right\}_j^i = \left\{\left\{\frac{dF(x)}{dx_k}\right\}_j - \left\{\frac{dP(\sigma_j^{i-1},x)}{dx_k}\right\}_j^{i-1}\right.$$

$$\left. - \left[\frac{d}{dx_k}\left[K_T(U_j^{i-1},x)\right]\right]_j^{i-1}\{\Delta U\}_j^i\right\} \tag{3.15}$$

Equation 3.10 and Equation 3.15 are in parallel with Equation 3.4 and Equation 3.6 of the elastic linear case, respectively. Equation 3.15 is similar to Equation 3.10, except for the change in the right hand side. Therefore, Equation 3.15 can be considered as another load case for Equation 3.10. The solution of Equation 3.15 will yield the gradients of the incremental displacements. The matrix Equation 3.15 can be solved by making use of the available factored global tangent stiffness matrix from the analysis phase (solution of Equation 3.10). The gradients of the incremental displacements are related to the gradients of the incremental stresses by differentiating Equation 3.13 as

$$\left\{\frac{d\ \Delta\sigma}{dx_k}\right\}_j^i = \left[\frac{dE_T(u_j^{i-1},x)}{dx_k}\right]_j^{i-1} [B]\ \{\Delta u\}_j^i$$

$$+ \left[E_T(u_j^{i-1},x)\right]_j^{i-1} [B]\left\{\frac{d\ \Delta u}{dx_k}\right\}_j^i \quad (3.16)$$

where $\{d\ \Delta u/dx_k\}_j^i$ is a subset of $\{d\ \Delta U/dx_k\}_j^i$.

At the end of each iteration, the gradients of incremental displacements and stresses are updated to form the new total gradients. The updating procedure is formulated by differentiating Equation 3.12 and Equation 3.14 as

$$\left\{\frac{dU}{dx_k}\right\}_j^i = \left\{\frac{dU}{dx_k}\right\}_j^{i-1} + \left\{\frac{d\ \Delta U}{dx_k}\right\}_j^i \quad (3.17)$$

and

$$\left\{\frac{d\sigma}{dx_k}\right\}_j^i = \left\{\frac{d\sigma}{dx_k}\right\}_j^{i-1} + \left\{\frac{d\ \Delta\sigma}{dx_k}\right\}_j^i \quad (3.18)$$

The complete gradient analysis can be summarized by the iterative solution of Equation 3.15 to Equation 3.18.

3.4.3. Evaluation of gradient equation

The right hand side vector of gradient Equation 3.15 can be obtained by using the updated displacement and stress derivative from the previous iteration, i.e., $\{dU/dx_k\}_j^{i-1}$ and $\{d\sigma/dx_k\}_j^{i-1}$. The left hand side of Equation 3.15 is the same as the left hand side of Equation 3.10. The term by term evaluation of the right hand side vector of Equation 3.15 is shown below.

• The term $\{dF(x)/dx_k\}_j$ is a zero vector unless $\{F(x)\}$ is a function of the basic variables, e.g., the applied force is a random variable or the force is a function of the random element geometry.

• The derivative of the internal force vector, $\{dP(\sigma_j^{i-1},x)/dx_k\}_j^{i-1}$ can be obtained by differentiating the Equation 3.11:

$$\left\{\frac{dP(\sigma_j^{i-1},x)}{dx_k}\right\}_j^{i-1} = \sum_{1}^{NE} \frac{d}{dx_k} \int_V [B]^T\{\sigma\}_j^{i-1}\, dv \qquad (3.19)$$

where the sum represents an assemblage of the elemental quantities into the structural vector. The updated total stress gradients from the previous iteration are used in Equation 3.19.

• The third term of the right hand side of Equation 3.15 is obtained by first obtaining the derivative of the global stiffness matrix, i.e., $\left[d/dx_k \left[K_T(u_j^{i-1}, x) \right]_j^{i-1} \right]$ and post-multiplying by the incremental displacement vector $\{\Delta U\}_j^i$. The vector $\{\Delta U\}_j^i$ is from the solution of Equation 3.10. The matrix $[d/dx_k\ [K_T(U_j^{i-1}, x)]]_j^{i-1}$ can be obtained by assembling the derivative of the element tangent stiffness matrices (similar to Equation 3.7). In nonlinear analyses, the element tangent stiffness matrix is determined by knowing the tangent elastic modulus of the material within the element for the current state of strains. The tangent modulus of elasticity is calculated from the uniaxial stress strain curve at the current total elemental effective strain, $\bar{\varepsilon}_j^{i-1}$. In the nonlinear elastic case, $\bar{\varepsilon}$ can be expressed in terms of strain components, $\{\varepsilon\}$, as (5, Chapter 13):

$$\bar{\varepsilon} = \left[\frac{\sqrt{2}}{2(1 + \nu)} \right] \left[(\varepsilon_x - \varepsilon_y)^2 + (\varepsilon_y - \varepsilon_z)^2 + (\varepsilon_z - \varepsilon_x)^2 + 1.5(\gamma_{xy}{}^2 + \gamma_{yz}{}^2 + \gamma_{zx})^2 \right]^{1/2}$$

$$= \bar{\varepsilon}\ (\{\varepsilon\}) \qquad (3.20)$$

Thus, the element stiffness matrix is a function of the current total elemental effective strain ($\bar{\varepsilon}_j^{i-1}$) as well as the basic variable (x). The derivative of the elemental tangent stiffness can be written as

$$\left[\frac{dk_T}{dx_k}\right]_j^{i-1} = \left[\frac{\partial k_T}{\partial \bar{\varepsilon}_j^{i-1}}\right]_j^{i-1} \left(\frac{d\bar{\varepsilon}_j^{i-1}}{dx_k}\right) + \left[\frac{\partial k_T}{\partial x_k}\right]_j^{i-1} \qquad (3.21)$$

The effective strain $\bar{\varepsilon}$ is related to the strain components, $\{\varepsilon\}$, of the element, e.g., Equation 3.20, which are related to the nodal displacements of the element as

$$\bar{\varepsilon}_j^{i-1} = \bar{\varepsilon}\left(\{\varepsilon\}_j^{i-1}\right) = \bar{\varepsilon}\left([B]\{u\}_j^{i-1}\right) \qquad (3.22)$$

The term $(d\bar{\varepsilon}_j^{i-1}/dx_k)$ is obtained by differentiating Equation 3.22 as

$$\left(\frac{d\bar{\varepsilon}_j^{i-1}}{dx_k}\right) = \bar{\varepsilon}\left([B]\left[\frac{du}{dx_k}\right]_j^{i-1}\right) \qquad (3.23)$$

where $[du/dx_k]_j^{i-1}$ is the elemental subset of the updated displacement gradient $[dU/dx_k]_j^{i-1}$.

3.5. Solution Algorithm

The procedure for the gradient analysis along with the nonlinear finite element analysis is given below. Suppose that $\{x\}$, $\{U\}_j^{i-1}$, $\{\sigma\}_j^{i-1}$, $\{P\}_j^{i-1}$, $\{F\}_j$, $\left[\frac{dU}{dx_k}\right]^{i-1}$, and $\left[\frac{d\sigma}{dx_k}\right]_j^{i-1}$ are given at the j^{th} load increment and the i^{th}

iteration. The condition $i=1$ and $j=1$ is the initial stage of the nonlinear problem. The total load is applied in increments of [ΔF] and the analysis steps follow:

1. Form the global stiffness matrix, $[K_T]_j^{i-1}$.
2. Factorize the global stiffness matrix, using Cholesky method (1).
3. Solve for the incremental displacements, $\{\Delta U\}_j^i$ (Equation 3.10).
4. Determine the incremental elemental stresses, $\{\Delta\sigma\}_j^i$ by Equation 3.13.
5. For a basic variable x_k, determine the right-hand side vector of Equation 3.15. The updated displacement and stress derivatives from the previous iteration (i-1) will be used. For details refer to Section 3.4.3.
6. Solve for the incremental displacement gradients $\{d\ \Delta U/dx_k\}_j^i$ by Equation 3.13. Note that the factored global stiffness matrix from Step 2 is used in the solution of Equation 3.15.
7. Find the incremental stress gradients, $\{d\ \Delta\sigma/dx_k\}_j^i$ by Equation 3.16 for all the elements.
8. Update gradients by Equations 3.17 and 3.18.
9. If all the basic variables are not considered, go to Step 5.
10. Update the nodal displacements and the elemental stresses (Equations 3.12 and 3.14).

11. Assemble the vector of internal forces $\{P\}_j^i$ by Equation 3.11. Determine the vector of unbalanced force, $\{\{F\}_j - \{P\}_j^i\}$.
12. Test for convergence. The convergence in this study is considered to be achieved if the Euclidean norm of the unbalanced force vector is less than a specified value. The Euclidean norm of a vector is the square root of the sum of the squares of the vector components (geometrically, this norm is the length of the vector). If the convergence is not satisfied, go to Step 1 with i replacing i-1.
13. Repeat Steps 1 to 12 for all the load steps. The final $\{U\}$, $\{\sigma\}$, $[dU/dx]$ and $[d\sigma/dx]$ is obtained by summing the results from all the load steps.

3.6. Summary

The Newton-Raphson iteration technique is proposed for the nonlinear structural analysis. The equilibrium equation is differentiated in each iteration and solved to find the gradients of the incremental displacements and stresses. At the end of each iteration, displacements and stresses are updated. An analogous procedure is used to update the incremental gradients. The current state of total displacement, total stress and material properties are used in formulating the equilibrium equation for the next iteration. Similarly, differentiation of the equilibrium equations in the next iteration is carried out by using the current state of the gradients. Hence, parallel to a common nonlinear structural analysis, gradient analysis is performed in each iteration and updated to find the final displacement and stress gradients. An optimizer may use this method in finding the gradients of some constraint function of interest with respect to a design variable. In this work, gradients will be used to find an approximate expression for the limit state. This approximate surface will be called a response surface.

4. GRADIENT ANALYSIS OF PLANE TRUSSES

4.1. Introduction

The procedure developed in Chapter 3 is applied here to find the displacement and stress gradients in a two-dimensional truss analysis. The nonlinearity of the material behavior is modeled by a modified Ramberg-Osgood equation. The area of the cross section, yield stress, Young's modulus and the shape parameter of the stress strain curve of all the truss members are considered as the independent basic variables. The solution algorithm outlined in Section 3.5 is implemented in a FORTRAN computer program to obtain the response gradients with respect to the basic variables. In the example problems, the results of the derivatives are confirmed by the closed form solutions wherever possible and, if not possible, by other numerical techniques.

4.2. Material Model Idealization

The modified Ramberg-Osgood equation is used to represent the stress-strain relationship (30):

$$\sigma = \frac{E_o \, \varepsilon}{\left[1 + \left| \frac{E_o \varepsilon}{\sigma_y} \right|^n \right]^{1/n}} \tag{4.1}$$

where σ, ε, E_o, σ_y and n are the stress, strain, initial Young's modulus, yield stress and shape factor, respectively. The above equation is represented in Figure 8. The tangent modulus E_T can be obtained by differentiating Equation 4.1 with respect to ε. E_T is given by

$$E_T = \frac{d\sigma}{d\varepsilon} = \frac{E_o}{\left[1 + \left|\frac{E_o \varepsilon}{\sigma_y}\right|^n\right]^{n+1/n}} \tag{4.2}$$

4.3. Structural Analysis

The structural analysis is done by the iterative solutions of Equations 3.10 through 3.14. In two-dimensional truss problems, the element tangent stiffness matrix in local coordinates at the jth load increment and ith iteration is given by

$$[k_T]_j^{i-1} = \frac{AE_o}{L[1 + T]^{n+1/n}} \begin{bmatrix} 1 & -1 \\ -1 & 1 \end{bmatrix} \tag{4.3}$$

where $$T = \left|\frac{E_o \varepsilon_j^{i-1}}{\sigma_y}\right|^n.$$

A is the area of the element, L is the length of the element, and ε_j^{i-1} is the current total strain of the element at the beginning of the i^{th} iteration of the j^{th} load increment. The

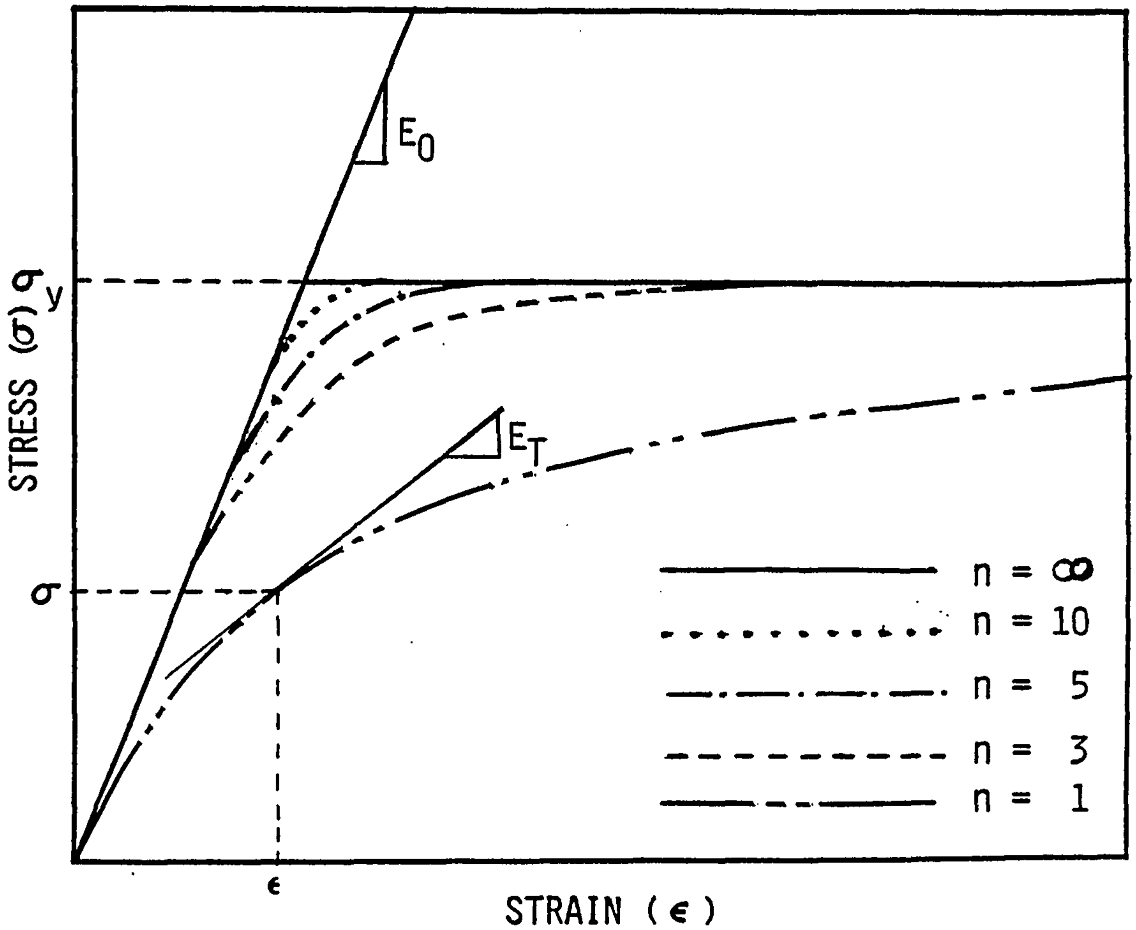

Figure 8. Modified Ramberg-Osgood equation

current total internal force $\{P\}_j^{i-1}$, as given in Equation 3.11, can be written

$$\{P\}_j^{i-1} = \sum_{1}^{NE} \{A\sigma_j^{i-1}\} \qquad (4.4)$$

where σ_j^{i-1} is the total stress which can be directly obtained from Equation 4.1 for the current ε_j^{i-1}. Since geometric nonlinearity is not considered, the elemental total strain can be directly related to the total nodal displacement u_1 and u_2 in local coordinates by

$$(\varepsilon_j^{i-1}) = \frac{1}{L}[1 \ -1] \begin{Bmatrix} u_1 \\ u_2 \end{Bmatrix} \qquad (4.5)$$

In this uniaxial stress case, updating the stresses is avoided because the current stress is uniquely related to the current total strain.

4.4. Gradient Analysis

The solution of Equation 3.15 will yield the derivatives of the nodal incremental displacements which then are updated to obtain the derivatives of the total displacement (Equation 3.17). The gradients of the total displacement are related to the derivatives of the total stress. The evaluation of the terms in Equation 3.15 is shown in this section. For each truss member, the areas of the cross section, yield stress, Young's modulus and the shape parameter of the stress strain curve are considered to be basic random variables.

4.4.1. Derivative of applied forces

In this study, the applied forces are considered to be neither basic variables nor functions of the basic variables. Therefore, $\{dF/dx_k\}_j$ is considered as zero vector.

4.4.2. Derivative of the global stiffness matrix

The derivative of the global stiffness matrix is multiplied by the incremental displacement vector in Equation 3.15. This can be achieved by differentiating only the element stiffness of the member associated with x_k. The differentiated elemental stiffness matrix is then multiplied by the elemental incremental nodal displacement vector $\{\Delta u\}_j^i$. The resulting 2 x 1 vector is then assembled to form the global vector which gives $[d/dx_k[K_T]]\{\Delta U\}_j^i$.

The differentiation of the elemental stiffness matrix is carried out by using Equation 3.21. Since the truss elements are under uniaxial stress state, the elemental effective strain ($\bar{\varepsilon}$) is equal to the total strain in the element (ε). Therefore, Equation 3.21 is written as

$$\left[\frac{dk_T}{dx_k}\right]_j^{i-1} = \left[\frac{\partial k_T}{\partial \varepsilon_j^{i-1}}\right]_j^{i-1} \left(\frac{d\varepsilon_j^{i-1}}{dx_k}\right) + \left[\frac{\partial k_T}{\partial x_k}\right]_j^{i-1} \qquad (4.6)$$

in which $[\partial k_T/\partial\varepsilon_j^{i-1}]_j^{i-1}$ is obtained by the differentiation of Equation 4.3, i.e.,

$$\left[\frac{\partial k_T}{\partial\varepsilon_j^{i-1}}\right] = \frac{-(n+1)\ AE_o\ (E_o\varepsilon_j^{i-1}/\sigma_y)\ \mathrm{Sgn}(\varepsilon_j^{i-1})}{L\sigma_y\ [1+T]^{(2n+1)/n}} \begin{bmatrix} 1 & -1 \\ -1 & 1 \end{bmatrix} \tag{4.7}$$

where $\mathrm{Sgn}(\varepsilon_j^{i-1}) = 1.0$ if $\varepsilon_j^{i-1} > 0$

$= -1.0$ if $\varepsilon_j^{i-1} < 0$

The term $(d\varepsilon_j^{i-1}/dx_k)$ in Equation 4.6 is obtained by differentiating Equation 4.5, i.e.,

$$\frac{d\varepsilon_j^{i-1}}{dx_k} = \frac{1}{L}\,[1,\ -1] \begin{Bmatrix} du_1/dx_k \\ du_2/dx_k \end{Bmatrix}_j^{i-1} \tag{4.8}$$

where du_1/dx_k and du_2/dx_k are the components of the vector $\{dU/dx_k\}$. The last term in Equation 4.6 is dependent upon the basic variable under consideration and evaluated by differentiating $[k_T]$ in Equation 4.3 with respect to x_k.

Case 1: $x_k = A$ = Area of the element

$$\left[\frac{\partial k_T}{\partial A}\right]_j^{i-1} = \frac{1}{A}\,[k_T]_j^{i-1} \tag{4.9}$$

Case 2: $x_k = \sigma_y$ = yield stress of the element

$$\left[\frac{\partial k_T}{\partial\sigma_y}\right]_j^{i-1} = \frac{(n+1)\qquad AE_o\ T}{\sigma_y\ [1+T]^{(2n+1)/2}} \begin{bmatrix} 1 & -1 \\ -1 & 1 \end{bmatrix} \tag{4.10}$$

Case 3: $x_k = E_o$ = Initial elastic modulus

$$\left[\frac{\partial k_T}{\partial E_o}\right] = \frac{A}{L}\frac{[1 - nT]}{[1 + T]^{(2n+1)/n}} \begin{bmatrix} 1 & -1 \\ -1 & 1 \end{bmatrix} \qquad (4.11)$$

Case 4: $x_k = n$ = shape factor

$$\left[\frac{\partial k_T}{\partial n}\right] = \frac{AE_o}{L\, n(1+T)^{(n+1)/n}} \left(\frac{\ln(1+T)}{n} - \frac{(n+1)T \ln\left|E_o \varepsilon^{i-1}/\sigma_y\right|}{(1 + T)}\right) \begin{bmatrix} 1 & -1 \\ -1 & 1 \end{bmatrix} \qquad (4.12)$$

4.4.3. Derivative of the internal force

The derivative of the internal force $\{P\}_j^{i-1}$ is obtained by differentiation of Equation 4.4, i.e.,

$$\left\{\frac{dP}{dx_k}\right\}_j^{i-1} = \sum_1^{NE} \left(\frac{dA}{dx_k}\right) \sigma_j^{i-1} + A\left(\frac{d\sigma_j^{i-1}}{dx_k}\right) \qquad (4.13)$$

the stress in each element is based upon the total strain (Equation 4.1). The derivative of the stress can be written as

$$\left(\frac{d\sigma}{dx_k}\right)_j^{i-1} = \left(\frac{\partial \sigma_j^{i-1}}{\partial \varepsilon_j^{i-1}}\right)\left(\frac{d\varepsilon_j^{i-1}}{dx_k}\right) + \left(\frac{\partial \sigma_j^{i-1}}{\partial x_k}\right) \qquad (4.14)$$

where $\left(\partial\sigma_j^{i-1}/\partial\varepsilon_j^{i-1}\right)$ is the tangent modulus (E_T) of the element as given by Equation 4.2, and $d\varepsilon_j^{i-1}/dx_k$ is given by Equation 4.8. The term $\partial\sigma_j^{i-1}/\partial x_k$ depends on the basic variable under consideration and is given by differentiating Equation 4.1 with respect to x_k.

Case 1: $x_k = A$

$$\frac{\partial \sigma_j^{i-1}}{\partial A} = 0 \tag{4.15}$$

Case 2: $x_k = \sigma_y$

$$\frac{\partial \sigma_j^{i-1}}{\partial \sigma_y} = \frac{E_o \varepsilon_j^{i-1}}{\sigma_y} \quad \frac{T}{[1 + T]^{(n+1)/n}} \tag{4.16}$$

Case 3: $x_k = E_o$

$$\frac{\partial \sigma_j^{i-1}}{\partial E_o} = \frac{\varepsilon_j^{i-1}}{[1 + T]^{(n+1)/n}} \tag{4.17}$$

Case 4: $x_k = n$

$$\frac{\partial \sigma_j^{i-1}}{\partial n} = \frac{E_o \varepsilon_j^{i-1}}{n(1+T)^{1/n}} \left(\frac{\ln(1+T)}{n} - \frac{T \ln \left| E_o \varepsilon_j^{i-1}/\sigma_y \right|}{(1 + T)} \right) \tag{4.18}$$

4.5. Examples

A FORTRAN program was written to implement the solution algorithm given in Section 3.5 for two-dimensional trusses. The factored global stiffness matrix, assembly routine, solution routine and updating procedures from the structural analysis are used in the gradient analysis. Four examples are analyzed. In three cases, the gradient results are compared with closed form solutions. In the last problem, the gradients are checked by the central difference method.

4.5.1. Example 1: Single bar problem

A single bar with one degree of freedom is analyzed. The geometry and the material properties are shown in Figure 9. The force-displacement relationship is obtained by modifying Equation 4.1:

$$U = \frac{QL}{AE_o[1 - (P/\sigma_y A)^n]^{1/n}} \tag{4.19}$$

where Q and P are the external and internal forces, respectively. In this example, Q is taken as 100 units. The stress in the element σ is given by

$$\sigma = Q/A \tag{4.20}$$

The exact derivatives of U and σ, with respect to variables A, σ_y, E_o and n, are obtained by differentiating Equations 4.19 and 4.20:

$$\frac{dU}{dA} = \frac{-QL}{A^2E_o}\left(\frac{1}{[1 - (P/\sigma_y A)^n]^{1/n}} + \frac{(P/\sigma_y A)^n}{[1 - (P/\sigma_y A)^n]^{(n+1)/n}}\right) \tag{4.21a}$$

$$\frac{dU}{d\sigma_y} = -\left(\frac{QL}{AE_o\sigma_y}\right)\left(\frac{P}{A\sigma_y}\right)^n \frac{1}{[1 - (P/\sigma_y A)^n]^{(n+1)/n}} \tag{4.21b}$$

$$\frac{dU}{dE_o} = \frac{-U}{E_o} \tag{4.21c}$$

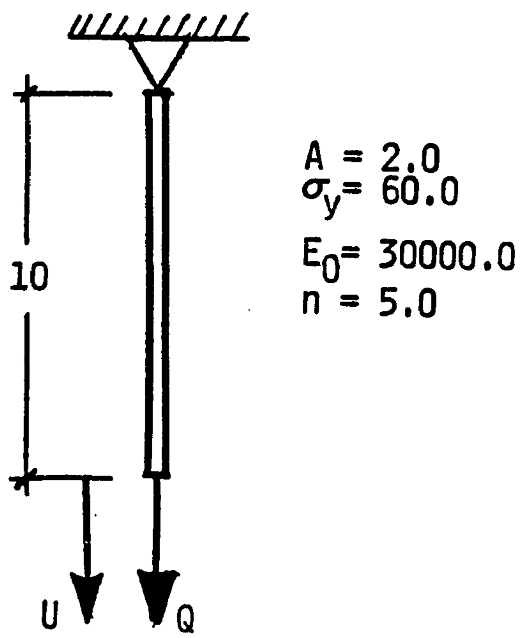

Figure 9. Single bar problem

$$\frac{dU}{dn} = \frac{QL}{AE_o} \frac{1}{n[1-(P/\sigma_y A)^n]^{1/n}} \left\{ \frac{(P/\sigma_y A)^n \ln(P/\sigma_y A)}{[1-(P/\sigma_y A)^n]} + \frac{1}{n} \ln[1-(P/\sigma_y A)^n] \right\} \tag{4.21d}$$

$$\left.\begin{aligned} \frac{d\sigma}{dA} &= -\frac{Q}{A^2} \\ \frac{d\sigma}{d\sigma_y} &= \frac{d\sigma}{dE_o} = \frac{d\sigma}{dn} = 0.0 \end{aligned}\right\} \tag{4.22}$$

The exact solutions for the displacement and stress are obtained by the solutions of Equations 4.19 and 4.20, respectively. The exact derivatives of displacement and stresses are calculated by using Equations 4.21 and 4.22. These results are tabulated in Table 1.

The finite element and gradient analysis procedure which is proposed in this work is used in finding the displacement as well as stress, and their gradients. A total load of 100 units is applied in five steps. The convergence in each step is considered to be achieved when the norm of the unbalanced force vector is less than the tolerance limit of 0.001 units. The results are tabulated in Table 1.

To study the effect of tolerance limit, the above problem is considered. A load of 119.8 is applied in 10 load steps to study the effect of tolerance limit in highly nonlinear region. The tolerance limit is varied and the results of

Table 1. One bar problem

	Exact	Newton-Raphson
U	0.01847101	0.01847101
σ	50.0	50.0
dU/dA	-0.154408E-1	-0.154408E-1
$dU/d\sigma_y$	-0.206844E-3	-0.206844E-3
dU/dE_o	-0.615701E-6	-0.615701E-6
dU/dn	-0.832280E-3	-0.832280E-3
$d\sigma/dA$	-25.0	-25.0
$d\sigma/d\sigma_y$	0.0	-0.150283E-8
$d\sigma/dE_o$	0.0	-0.216840E-8
$d\sigma/dn$	0.0	-0.423710E-9

displacements and its gradients are plotted (Figure 10). When compared to displacement and stresses, the gradients are most vulnerable to the relaxation of the tolerance limit. This is to be expected since the gradients are the derivatives of the displacements and the stresses. In the remainder of the examples, the tolerance limit is kept as 0.001 and the analysis is carried out.

4.5.2. Example 2: Two bars in parallel

The geometry and the material properties of two bars in parallel are shown in Figure 11. In this indeterminate system, the bar forces (P_1, P_2) depend on the displacement. The following set of equations are solved iteratively to find the displacement:

$$U = \frac{Q}{\frac{A_1E_1}{L_1}\left[1-\left(\frac{P_1}{A_1\sigma_{y_1}}\right)^{n_1}\right]^{1/n_1} + \frac{A_2E_2}{L_2}\left[1-\left(\frac{P_2}{A_2\sigma_{y_2}}\right)^{n_2}\right]^{1/n_2}} \qquad (4.23)$$

where

$$P_1 = U\frac{A_1E_1}{L_1}\left[1-\left(\frac{P_1}{A_1\sigma_{y_1}}\right)^{n_1}\right]^{1/n_1} \qquad (4.24)$$

and

$$P_2 = Q - P_1 \qquad (4.25)$$

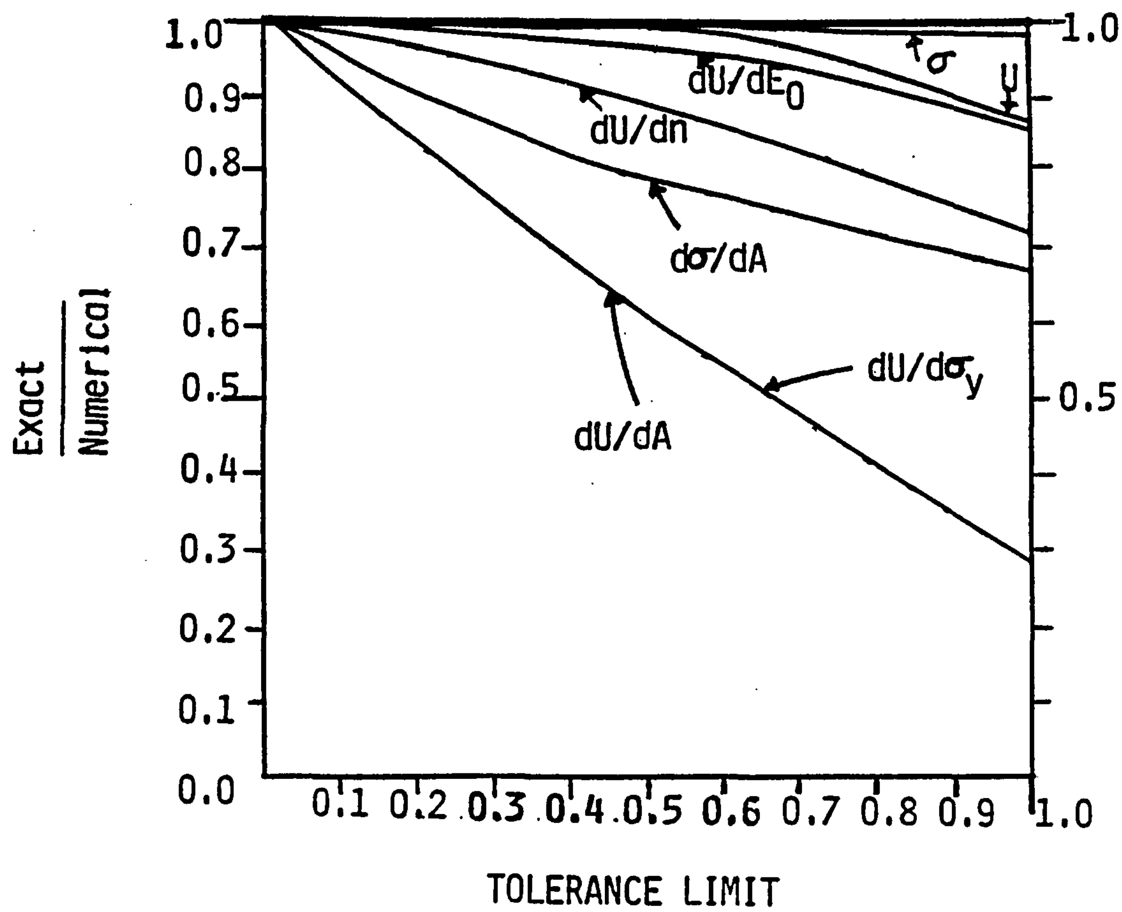

Figure 10. Convergence of displacements, stresses and its gradients

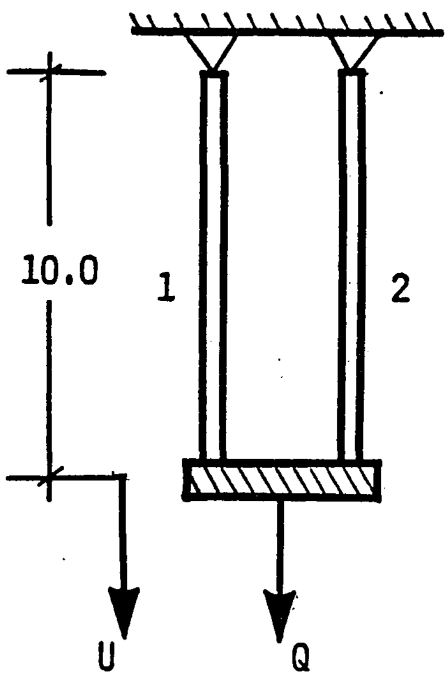

	Member 1	Member 2
A	2.0	4.0
σ_y	60.0	30.0
E_0	30000.0	10000.0
n	5.0	2.0

Figure 11. Two bars in parallel

A force (Q) of 200 units is applied. The exact stresses are computed by knowing the forces in the members, P_1 and P_2. In this example A, σ_y, E and n of Member 1 are considered as the basic variables. In order to obtain the gradients, Equations 4.23 and 4.24 are differentiated implicitly with respect to each basic variable x. This differentiation resulted in two expressions relating dP_1/dx and dU/dx. These two equations are then solved to obtain dU/dx and dP_1/dx. For example, let the basic variable be the Young's modulus of Member 1. Then, the differentiation of Equations 4.23 and 4.24 will result in the following equations.

$$\frac{dU}{dE_1} = -\frac{U^2}{F}\left\{\frac{A_1}{L_1}\left[1-\left(\frac{P_1}{A_1\sigma_{y_1}}\right)^{n_1}\right]^{1/n_1} - \frac{E_1}{L_1\sigma_{y_1}}\left(\frac{P_1}{A_1\sigma_{y_1}}\right)\frac{dP_1}{dE_1}\right.$$

$$\left[1-\left(\frac{P_1}{A_1\sigma_{y_1}}\right)^{2}\right]^{(1/n_1)-1} + \frac{A_2E_2}{L_2}\left(\frac{1}{A_2\sigma_{y_2}}\right)^{n_2}\left(Q-P_1\right)^{n_2-1}\frac{dP_1}{dE_1}$$

$$\left.\left[1-\left(\frac{Q-P_1}{A_2\sigma_{y_2}}\right)^{n_2}\right]^{(1/n_2)-1}\right\} \qquad (4.26)$$

$$\frac{dP_1}{dE_1} = \frac{dU}{dE_1} \cdot \frac{A_1E_1}{L_1}\left[1-\left(\frac{P_1}{A_1\sigma_{y_1}}\right)^{n_1}\right]^{1/n_1} + U\left\{\frac{A_1}{L_1}\left[1-\left(\frac{P_1}{\sigma_{y_1}A_1}\right)^{n_1}\right]^{1/n_1}\right.$$

$$\left. - \frac{E_1}{L\sigma_{y_1}} \cdot \frac{P_1}{A_1\sigma_{y_1}} \cdot \frac{dP_1}{dE_1} \cdot \frac{1}{\left[1-(P_1/A_1\sigma_{y_1})^{n_2}\right]^{1/n_2}}\right\} \qquad (4.27)$$

Equations 4.26 and 4.27 are solved to obtain dU/dE_1, and dP_1/dE_1. The stress gradients are calculated by knowing dP_1/dx. The results of displacements and its gradients using the closed form expressions are tabulated in Table 2.

The finite element procedure is used in evaluating the displacement, stresses and its gradients. Since, in the numerical procedure, dU/dx depends on $d\sigma/dx$, only the results of dU/dx are checked in Table 2. The load Q of 200 units is applied in five steps. The convergence in each load step is considered to be achieved when the norm of the unbalanced force vector is less than 0.001 units.

4.5.3. Example 3: Two bars in series

The two bars in Example 2 are arranged in series as shown in Figure 12. The displacements U_1 and U_2 are given by the following equations:

Table 2. Two bars in parallel

	Exact	Newton-Raphson
U	0.029013	0.029013
σ_1	58.28923	58.28885
σ_2	20.85579	20.85558
dU/dA_1	-0.28750E-1	-0.28757E-1
$dU/d\sigma_{y_1}$	-0.82940E-3	-0.82946E-3
dU/dE_1	-0.25823E-6	-0.25822E-6
dU/dn_1	-0.90921E-3	-0.90921E-3

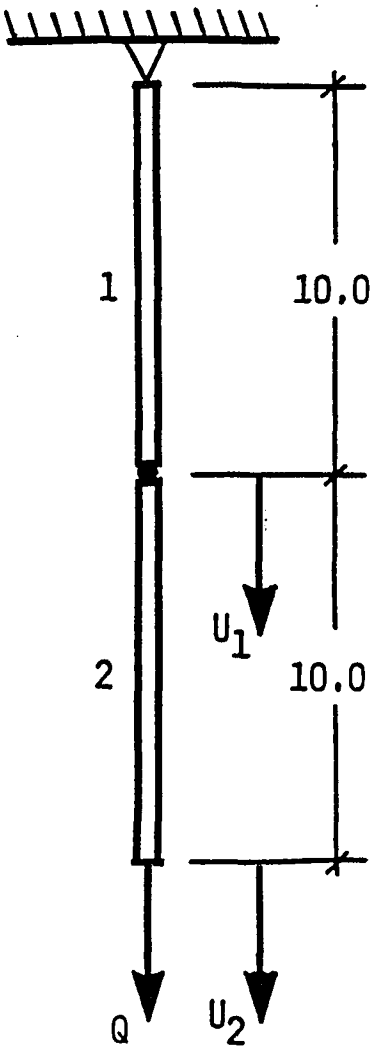

	Member 1	Member 2
A	2.0	4.0
σ_y	60.0	30.0
E_0	30000.0	10000.0
n	5.0	2.0

Figure 12. Two bars in series

$$U_1 = \frac{QL_1}{A_1E_1\left[1-\left(P_1/\sigma_{y_1}A_1\right)^{n_1}\right]^{1/n_1}} \tag{4.28}$$

and

$$U_2 = \frac{QL_2}{A_2E_2\left[1-\left(P_2/\sigma_{y_2}A_2\right)^{n_2}\right]^{1/n_2}} + U_1 \tag{4.29}$$

where P_1 and P_2 are the bar forces and are equal to the applied load Q. The total applied load, Q, is equal to 100 units. The stresses in each bar can be obtained by dividing the bar forces by the corresponding area of the cross section. The area of the cross section of Element 1 and Element 2 are considered as basic variables. The derivatives of the displacements are obtained in closed form by differentiating the displacement expressions (Equations 4.28 and 4.29). The exact values of displacements and its gradients are tabulated in Table 3.

The nodal displacements and its derivatives are determined by the finite element technique. The results are tabulated in Table 3. The total load is applied in five steps and iterated until the norm of the unbalanced force vector is less than 0.001. The derivatives of the displacements with respect to other variables are checked but not tabulated. Note that

Table 3. Two bars in series

	Exact	Newton-Raphson
U_1	0.01847101	0.01847098
U_2	0.0636977	0.06369781
dU_1/dA_1	-0.01544083	-0.01544085
dU_1/dA_2	0.0	0.1525212E-13
dU_2/dA_1	-0.01544083	-0.01544085
dU_2/dA_2	-0.0370035	-0.03700373

dU_1/dA_2 is approximately zero, because the displacement U_1 is not affected by the change in A_2.

4.5.4. Example 4: Ten bar truss

This truss problem in Figure 13 has been presented in the literature as an example of system reliability computations (12, 13, 15). The dimensions of the members and material properties, as given by Gorman and Moses (13), are duplicated here and shown in Figure 13. The nonlinearity of the material behavior is modeled by taking n equal to 5 in the modified Ramberg-Osgood model (Equation 4.1).

The load versus the y-displacement of Node 3 for mean values of the basic parameters is plotted and shown in Figure 14. The areas of cross section of all the members are considered as the basic variables. The derivatives of displacements and stresses are evaluated for an applied load, Q, of 1.6 units. The load is applied in 10 steps. The gradient of the vertical nodal displacement at Nodes 3 and 4 and the gradients of the stress in Element 5 are tabulated in Table 4.

To check the result, the gradient of the y-displacement at Node 3 with respect to the cross-sectional area of Member 7 (A_7) is considered. The displacement is found by additional analyses with a perturbed value of the area of Member 7. The displacements are tabulated in Table 5. The derivative of the

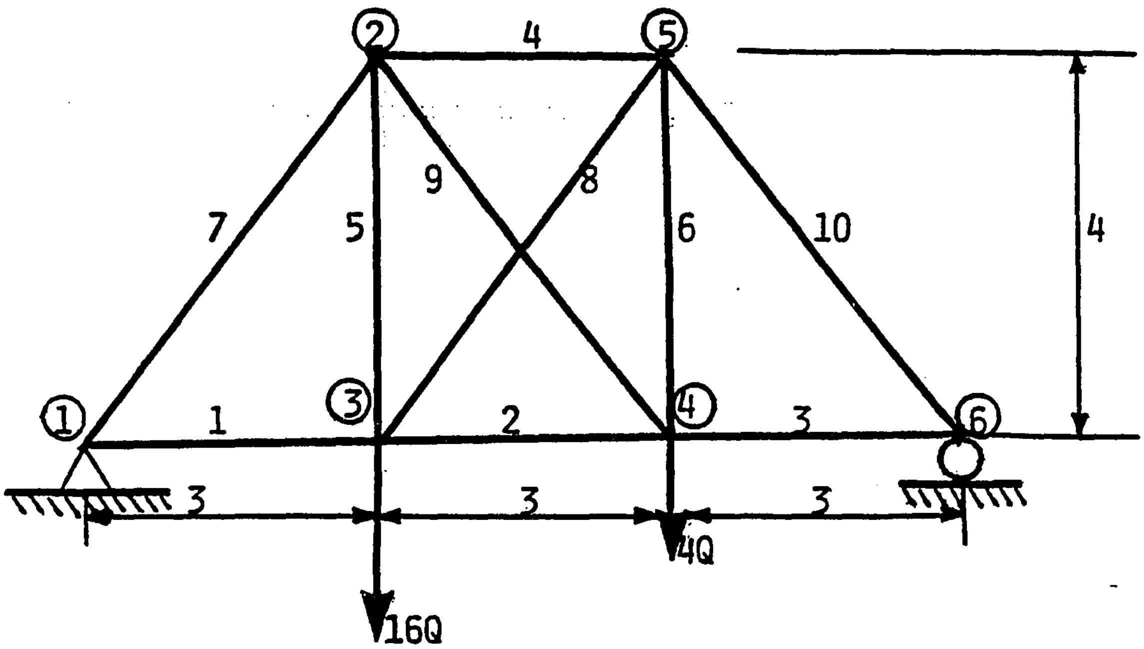

Element Number	Area of cross section A	Element Resistance $R=\sigma_y A$
1	0.3	15.0
2	0.3	15.0
3	0.3	15.0
4	0.3	15.0
5	0.4	20.0
6	0.4	20.0
7	0.5	25.0
8	0.2	10.0
9	0.2	10.0
10	0.5	25.0

$\sigma_y = 50.0$

$E_o = 30{,}000.0$

$n = 5.0$

Figure 13. Ten bar truss

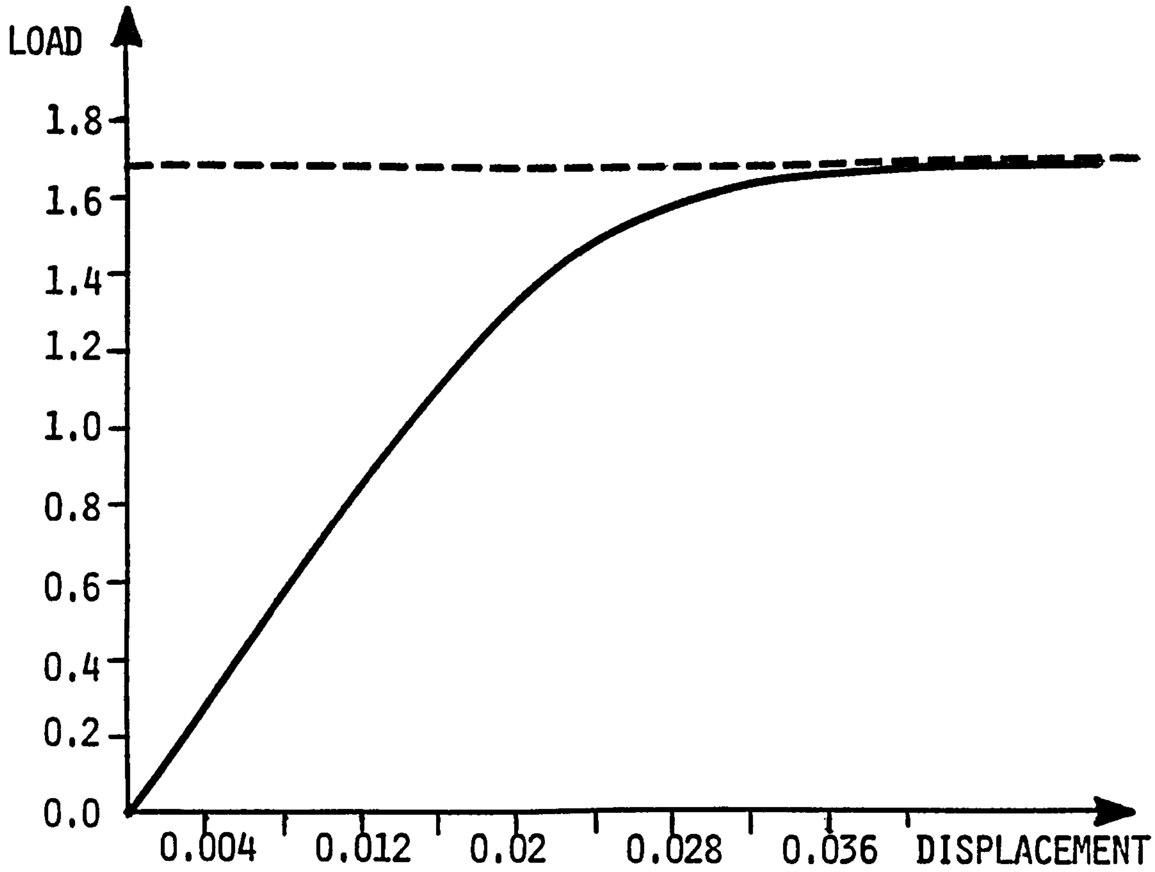

Figure 14. Load displacement curve of ten bar truss

Table 4. Displacement and stress gradients of ten bar truss

Member (i)	dU_{Y3}/dA_i	dU_{Y4}/dA_i	$d\sigma_5/dA_i$
1	-0.6074E-01	-0.3037E-01	-0.3355E-05
2	-0.2653E-02	-0.4255E-02	+0.2899E+01
3	-0.3056E-02	-0.6112E-02	-0.0000E+00
4	-0.5952E-01	-0.4506E-01	-0.2616E+02
5	-0.8290E-01	-0.1695E-01	-0.7850E+02
6	+0.2513E-03	-0.4292E-02	+0.1696E+01
7	-0.1013E+00	-0.5062E-01	-0.0000E+00
8	-0.2453E-01	+0.8189E-02	-0.2024E+02
9	+0.1931E-04	+0.8585E-04	+0.1303E+00
10	-0.5093E-02	-0.1019E-01	+0.6711E-05

U_{Y3} = Y-displacement of Node 3

U_{Y4} = Y-displacement of Node 4

σ_5 = Stress in the Element 5

Table 5. Vertical displacement of Node 3 for different values of area of Member 7

Grid Point	A_7	$U \times 10^{-1}$
0.5–3h	0.485	0.321319
0.5–2h	0.49	0.304701
0.5–h	0.495	0.295853
0.5	0.5	0.289904
0.5+h	0.505	0.285453
0.5+2h	0.51	0.281910
0.5+3h	0.515	0.278971

h = 0.005

displacement is approximated by using the central difference method (11).

$$\frac{dU}{dA_7} = \frac{1}{2h}\Bigg\{ U_{0.5+h} - U_{0.5-h} - 1/6\Big[U_{0.5+2h} - 2(U_{0.5+h} - U_{0.5-h}) - U_{0.5-2h}\Big] + 1/30\Big[U_{0.5+3h} + 4(U_{0.5-2h} - U_{0.5+2h}) + 5(U_{0.5+h} - U_{0.5-h})\Big] + \text{higher order terms}\Bigg\} \tag{4.30}$$

where h is the grid size and equal to 0.005. The displacement value at the cross-sectional area of 0.5+h is given by $U_{0.5+h}$. The displacement values are substituted into Equation 4.30 and dU/dA_7 is calculated. The calculated value of dU/dA_7, from Equation 4.30, is equal to -0.101743, which compares with the result of -0.1013 from the finite element technique (Table 4).

4.6. Conclusions

The displacement and stresses are calculated by using a nonlinear finite element technique. The gradients of the displacements and stresses with respect to the basic variables are evaluated in conjunction with the calculation of stresses and displacements. The procedure developed in Chapter 3 is applied to a plane truss problems. In four examples, the results for the displacements, stresses and their gradients are compared with the exact results. The results from the numerical procedure match very well with the exact results. This confirms the validity of the method. The main advantage in this method is that the gradients are exact (except for truncation and round off errors). The value of the gradients are shown to be convergent. Also, the gradient analysis is part of the nonlinear finite element analysis, i.e., the tangent stiffness matrices which are formulated and decomposed in the analysis phase are conveniently used for gradient computation.

5. ESTIMATION OF PROBABILITY OF FAILURE

5.1. Introduction

In this chapter, the response surface methodology is introduced to approximate the limit state function expressed in terms of the structural displacements. The finite element and gradient analysis developed in Chapters 3 and 4 determine the values and gradients of the failure surface. A piecewise linear approximation to the failure surface is constructed with these results. The Monte Carlo technique and AFOSM method are used to estimate the probability of failure.

5.2. Limit State Function

The limit state is that state beyond which the structure is considered to have failed. A limit state can be defined from a strength or a serviceability point of view. Here, the limit state is (refer to Chapter 1)

$$G_j = 1 - \left|U_{Qj}\right| / U_{Rj} , \qquad j = 1, \text{NDOF} \tag{5.1}$$

where $G_j = 0$ is the limit state surface which divides the "survival" and "failure" regions. The displacement of the j^{th} degree of freedom due to load, Q, is represented by U_{Qj}, and the term U_{Rj} is the limiting displacement of the j^{th} degree of freedom. The total number of degrees of freedom in the structure is denoted by NDOF. The structure is considered to have failed if $|U_{Qj}|$ is greater than U_{Rj}, i.e., G<0.

The derivative of the limit state function, with respect to a variable (x_k), is

$$\frac{dG_j}{dx_k} = -\frac{1}{U_{Rj}} \cdot \left(\frac{dU_{Qj}}{dx_k}\right) \cdot \mathrm{Sgn}(U_{Qj}) \qquad (5.2)$$

where $\mathrm{Sgn}\,(U_{Qj}) = -1$ if $U_{Qj} < 0$

$= 1$ if $U_{Qj} > 0$

The gradient of the displacement, dU_{Qj}/dx_k, in Equation 5.2 is obtained by the procedure outlined in Chapter 3 and applied to Chapter 4.

The limit state function, Equation 5.1, is formulated in such a way that the value of G_j is nondimensional. Therefore, the values of the different G's can be compared. Another advantage of such a limit state (Equation 5.1) is that it can be made to accommodate both ultimate and serviceability limit states. A typical serviceability limit state is that the deformation should not adversely affect the appearance or the efficiency of the structure (3). The ultimate limit states can be the loss of static equilibrium or excessive deformation. The loss of static equilibrium is the state when the system resistance (R) is less than the applied load (refer to Chapter 2). The probability of failure is defined as the probability that R is less than Q. This problem is equivalent to the problem of finding the probability that $U_Q > U_R$, where U_Q and U_R are the displacements at the load levels Q and R, respectively (Figure 15). The proof follows. Let the monotonic relationships between load and displacement be described by

$$U_R = h(R) \text{ and } U_Q = h(Q) \tag{5.3}$$

for U_R and U_Q, respectively. The function, h, represents the finite element solution, e.g., U_Q is the value of the displacement for load Q, as shown in Figure 15. The probability density function (p.d.f.) of U_Q can be obtained by transformation as (17, Chapter 5)

$$f_{U_Q} = \left|\frac{dQ}{dU_Q}\right| f_Q = \left|\frac{dh^{-1}(U_Q)}{dU_Q}\right| f_Q \tag{5.4}$$

where f_{U_Q} is the p.d.f. of U_Q. Similarly, the p.d.f. of U_R can be obtained as

$$f_{U_R} = \left|\frac{dh^{-1}(U_R)}{dU_R}\right| f_R \tag{5.5}$$

Now, by basic probability theory (refer to Chapter 2)

$$\Pr(U_R < U_Q) = \iint_{D(U_R<U_Q)} f_{U_Q}(u_Q)\, f_{U_R}(u_R)\, dU_R\, dU_Q \tag{5.6}$$

The above probability is shown in Figure 15. Substituting for

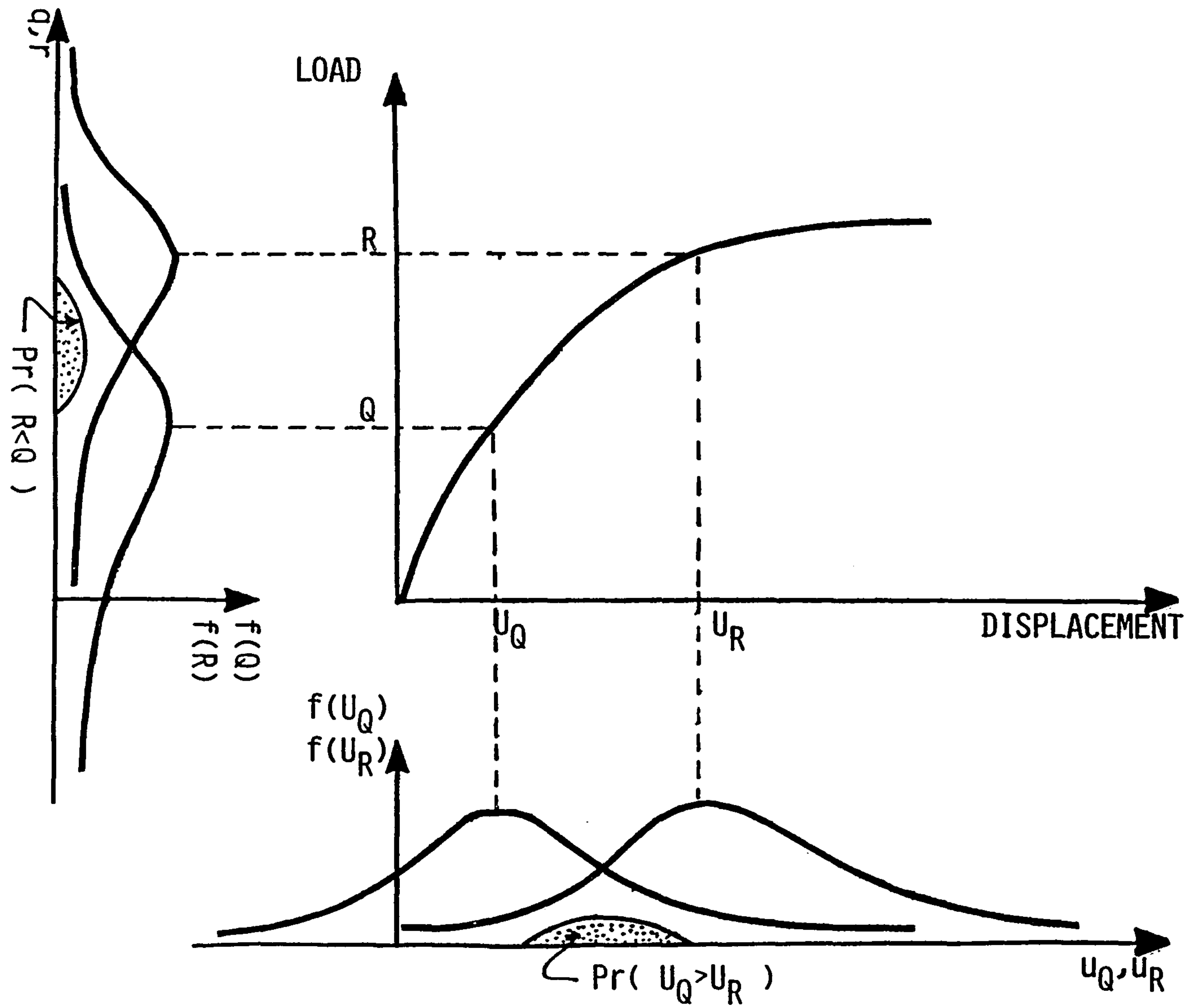

Figure 15. Transformation of resistance limit state to displacement limit state

f_{U_Q} and f_{U_R}, from Equations 5.4 and 5.5,

$$Pr(U_R < U_Q) = \iint_{D(U_R < U_Q)} f_Q(q)\ f_R(r) \left| dh^{-1}(U_Q)/dU_Q \right| dU_Q$$

$$\cdot \left| dh^{-1}(U_R)/dU_R \right| dU_R \tag{5.7}$$

$$= \iint_{D(R < Q)} f_Q(q)\ f_R(r)\ dr\ dq \tag{5.8}$$

The right hand side integral of the above equation is shown in Figure 15

$$Pr\ (U_R < U_Q) = Pr\ (R < Q) = p_f \tag{5.9}$$

which shows that the probability that the system reaches an ultimate state can be determined by the displacement limit state of Equation 5.1.

5.3. Advanced First Order Second Moment Method

The limit state function is defined in Equation 5.1 and its derivative with respect to variables can be obtained in Equation 5.2. Now, it is possible to use the AFOSM method to evaluate the probability of failure. A brief description of the method is given in Chapter 2. Here, the method will be explained in detail (4, 9, 22, 31). This explanation will also serve as the basis for the method which will be proposed in this work.

5.3.1. Reliability index

Let $\{x\}$ be the vector of basic random variables, assumed to be uncorrelated. The statistical character of each variable is described by its first two moments and distribution. The random variables, x_k, are transformed to a set of standardized variables, Y_k, with zero mean and unit variance as:

$$Y_k = \frac{x_k - \bar{x}_k}{\sigma_{x_k}} \tag{5.10}$$

where $\bar{x}_k$ is the mean value of x_k and σ_{x_k} is the standard deviation of x_k. If there was a correlation between x_k, expressed in terms of a known covariance matrix, it would always be possible to replace these variables by uncorrelated ones by means of an orthogonal transformation (22).

In the transformed space, the failure function is expressed as

$$G(Y_1,\ Y_2, \ldots Y_n) = 0 \tag{5.11}$$

For the case of two variables, the failure surface in the original coordinates and in the transformed space is shown in Figure 16.

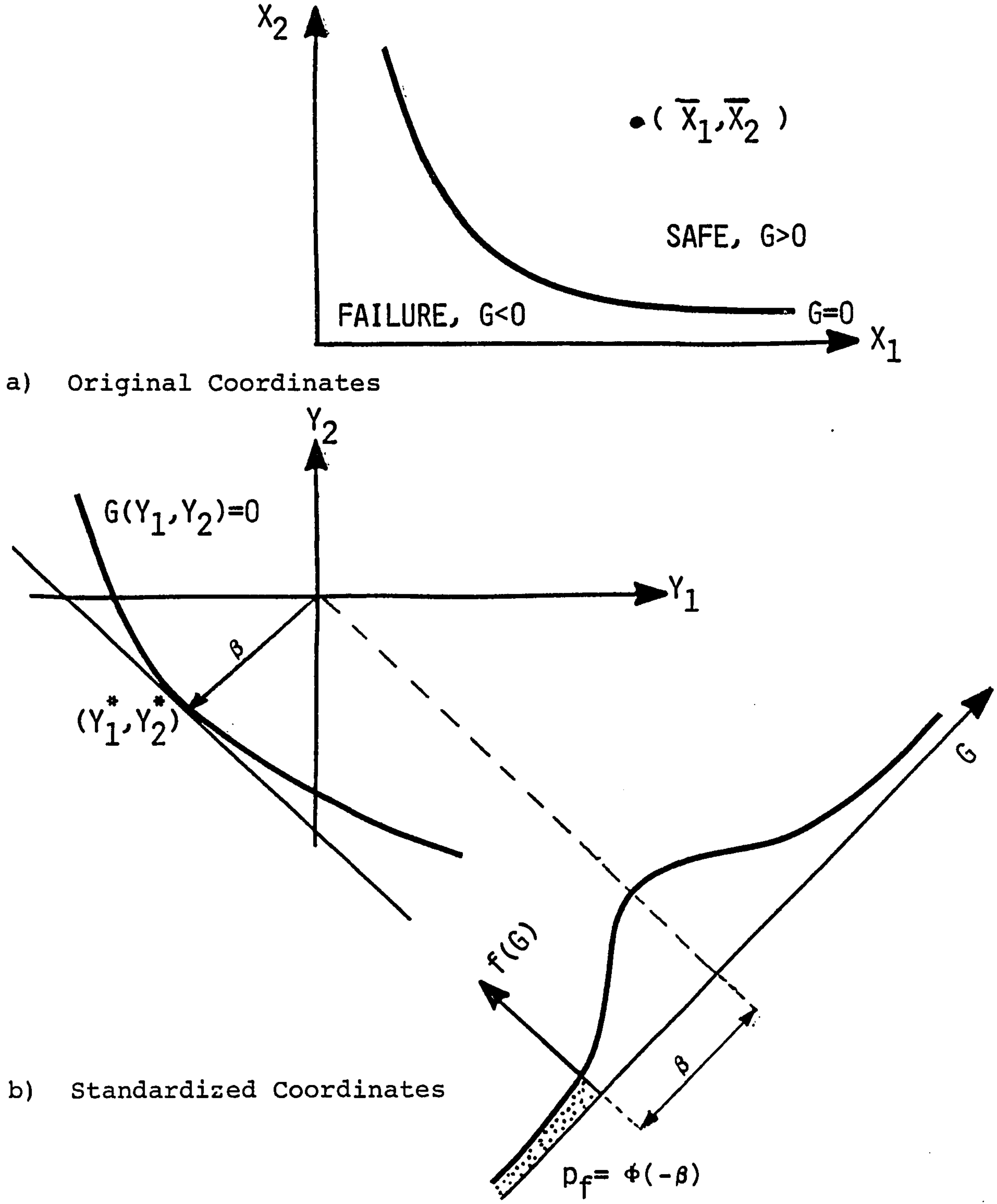

Figure 16. Advanced first order second moment method

The reliability index, β, is the minimum distance between the origin and the failure surface in the Y-space. The point on the failure surface corresponding to the minimum distance is represented by Y^* in Figure 16b. The probability of failure is approximated by (Figure 16)

$$p_f = \Phi\ (-\beta_{min}) \tag{5.12}$$

where Φ is the standard normal integral. The p_f calculated from Equation 5.12 yields an exact value of p_f if G = 0 is a linear function of Y_1 and Y_2. When G = 0 is nonlinear, as shown in Figure 16b, an error (p_f') would arise in p_f due to the linearization of the failure surface at Y^*. However, this error is proved to be minimum when the linearization of the failure surface is done at Y^* (4).

5.3.2. Solution for reliability index

The solution for the minimum β can be cast as an optimization problem, where the objective function is the distance from the origin to the point on the failure surface G(Y) = 0. To find the minimum distance β, the following minimization problem must be resolved:

Find $\{Y\}$, which will minimize

$$\beta^2 = \sum_1^N Y_k^2$$

subject to the constraint

$$G(Y_k) = 0.$$

The problem can be stated in terms of the original coordinates:

Find $\{x\}$, which will minimize

$$\beta^2 = \sum_{k=1}^{N} \left(\frac{x_k - \bar{x}_k}{\sigma_{x_k}} \right)^2$$

subject to

$$G(x_k) = 0.$$

Any nonlinear programming technique can be used to solve the above minimization problem (8). For one such method, an iterative scheme with the following set of equations will suffice:

$$x_k^* = \bar{x}_k - \alpha_k \beta \sigma_{x_k} \tag{5.13}$$

$$\alpha_k = \left.\frac{dG}{dx_k}\right|_{x_k^*} \cdot \sigma_{x_k} \Bigg/ \left[\sum_{i=1}^{N} \left(\left.\frac{dG}{dx_k}\right|_{x_k^*} \cdot \sigma_{x_k} \right)^2 \right]^{1/2} \tag{5.14}$$

$$G(x^*_k) = 0 \tag{5.15}$$

The quantities α_k are the direction cosines of the shortest vector from the origin to the failure surface in Y-space. The point x^*_k is referred to as "design point" or "failure point". The iterative procedure for solving these equations is explained later in this section.

When the probability distribution of a variable is non-normal, the distribution information is included by modifying its mean and standard deviation. The true distribution of each variable is matched to an equivalent normal distribution having the same probability density and cumulative tail area. Matching is done at the design point (x^*_k) in the original variable space. The mean $(\bar{x}^N_k)$ and standard deviation $(\sigma^N_{x_k})$ of the equivalent normal distribution are given by

$$\sigma^N_{x_k} = \frac{\phi\left(\Phi^{-1}\left[F_{x_k}(x^*_k)\right]\right)}{f_{x_k}(x^*_k)} \tag{5.16}$$

and

$$x^N_k = x^*_k - \Phi^{-1}\left[F_{x_k}(x^*_k)\right]\sigma^N_{x_k} \tag{5.17}$$

where ϕ and Φ are the standard normal density and cumulative distribution functions, and $F_{x_k}(.)$ and $f_{x_k}(.)$ denote the actual cumulative distribution and density distribution of the nonnormal variable, x_k.

The procedure for finding the minimum β contains the following steps.

1. Define the statistics of the basic variables. Define the limit state, G, of the form of Equation 5.1. Choose an initial value of the reliability index, β.
2. Set the initial design point, x^*_k, equal to the mean values, $\bar{x}_k$.
3. Begin iteration with $i = 1$.
4. Conduct finite element and gradient analysis at x^*_k (refer to Chapters 3 and 4) to evaluate the values of G and dG/dx_k, respectively. Values of G and dG/dx_k are evaluated using Equation 5.1 and 5.2, respectively.
5. If the variables are not normally distributed, calculate $\sigma^N_{x_k}$ and x^N_k, using Equations 5.16 and 5.17, respectively.
6. Compute α_k, using Equation 5.14 for all the variables. Note, if x_k is not normally distributed, $\sigma^N_{x_k}$ is used in Equation 5.14.
7. Calculate new values of x^*_k from Equation 5.13.
8. Repeat Steps 4 to 7 until convergence in x^*_k is achieved within specified limits.
9. Conduct finite element and gradient analysis at x^*_k. If the value of G is equal to zero within specified limits, go to Step 11.
10. Compute a new value of β,

$$\beta_{i+1} = \beta_i - G(\partial\beta/\partial G) \qquad (5.18)$$

Go to Step 4 by incrementing i by one.

11. The probability of failure is computed using Equation 5.12.

5.3.3. Multiple failure modes

In a structural problem, the overall failure may be defined by more than one failure mode or mechanism (Equation 5.1). The presence of multiple failure modes may decrease the overall reliability of the structure. As in Figure 17, the failure region is represented by the intersection of two limit states. For each mode of failure, $G_j(x)$, a reliability index, β_j, may be calculated by the AFOSM method, as outlined in Section 5.3.2. The probability of failure for each mode is determined by using Equation 5.12. One set of bounds on the probability of failure is defined by

$$\text{Max}\ (p_{f_j}) \leq p_f \leq \sum_{j=1}^{\text{Modes}} p_{f_j} \qquad (5.19)$$

The lower bound is associated with perfectly correlated failure modes and the upper bound with independent modes. For a large number of failure modes, the bounds will be very wide. The bounds suggested by Ditlevsen (7) can be employed, which account for dependence between the modes.

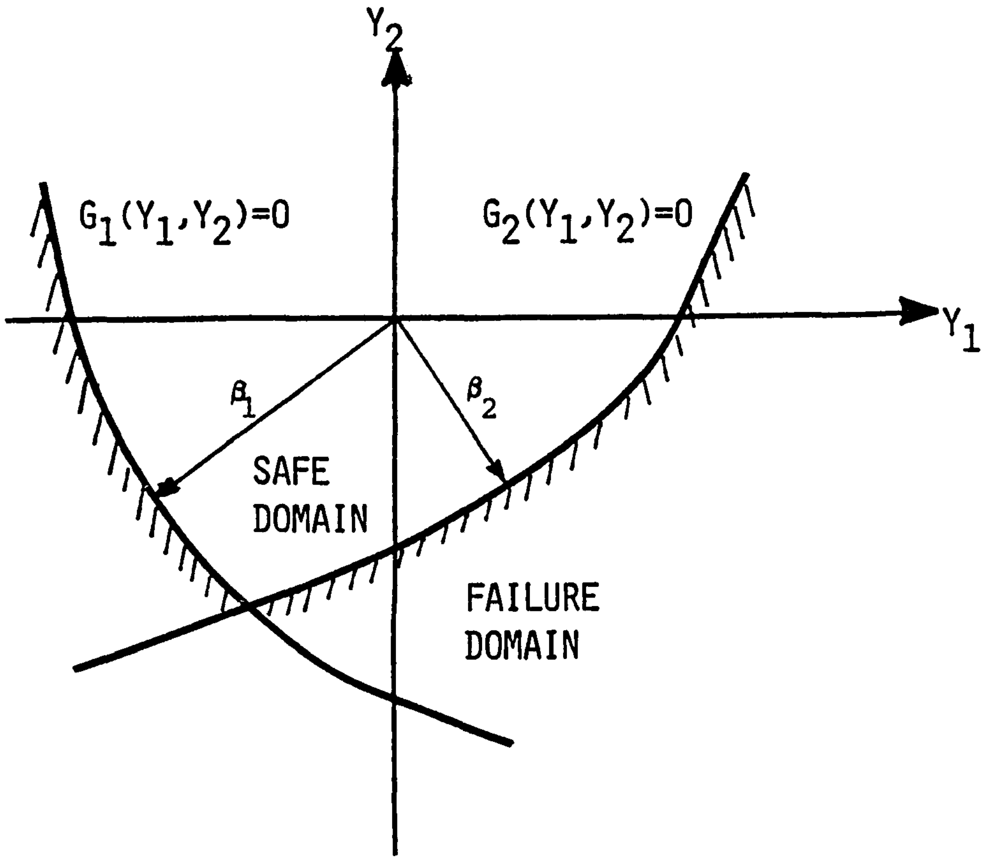

Figure 17. Multiple failure modes in AFOSM method

5.4. Response Failure Surface Method

5.4.1. A point on the failure surface

The analysis begins by finding a point on the failure surface $G(X) = 0$, preferably the point closest to the origin. At points closer to the origin, the coordinate of the probability density function of x, i.e., $f_x(x_1, x_2, \ldots x_N)$, is larger. To locate such a point, the following procedure is followed. As in the AFOSM method, the basic variables (x) will be transformed into the standardized variables (Y) for the response surface method (Equation 5.10). The limit state and its gradients are evaluated at a known point, A (Figure 18). Let the coordinates of point A be Y^E. The superscript E indicates that this point, A, is an expansion point. An expansion point is referred to a point where the values of G and dG/dx_k are evaluated. From these values, the limit state (G) is approximated by Taylor's series (Z) as

$$G \simeq Z = G\Big|_{Y^E} + \sum_{k=1}^{N} \frac{dG}{dY_k}\Big|_{Y^E}(Y_k - Y_k^E) \qquad (5.20)$$

where Z is the linearized surface. The equation for the hyper-plane, Z = 0, is written as

$$G\Big|_{Y^E} + \sum_{k=1}^{N} \frac{dG}{dY_k}\Big|_{Y^E}(Y_k - Y_k^E) = 0 \qquad (5.21)$$

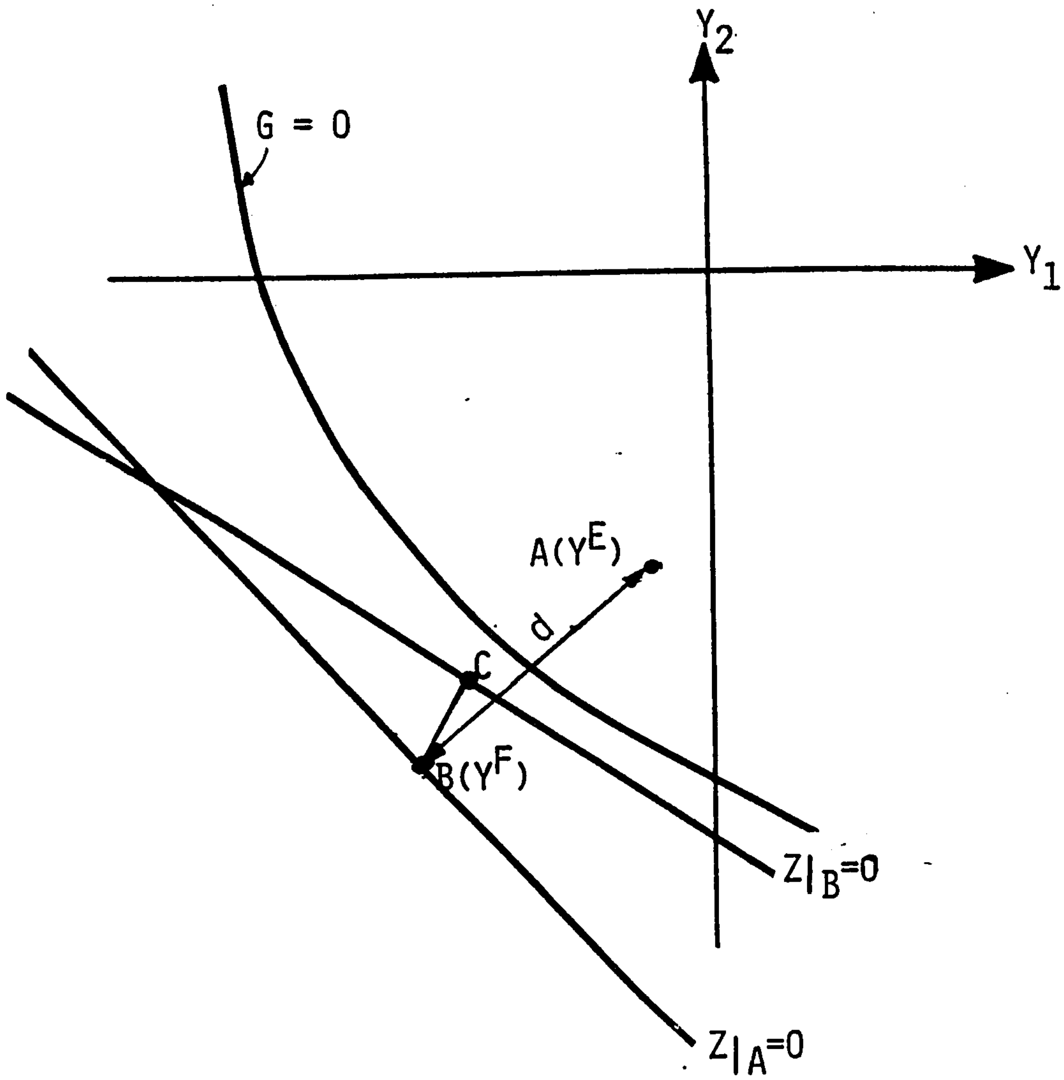

Figure 18. Obtaining a point on the failure surface G = 0

This plane is a straight line for the two variable case shown by $Z|_A = 0$ in Figure 18.

The point B is a point on the failure plane $Z|_A = 0$, which is at a minimum distance from point A. The coordinates of point B are designated as Y^F. The superscript indicates that this point is on a failure plane. The ordinate of B can be written as:

$$Y_k^F = Y_k^E - \alpha_k d \qquad (5.22)$$

where the α_k are the direction cosines of the limit state function evaluated at Y^E, and written as

$$\alpha_k = \left(\frac{dG}{dY_k}\right)\Bigg|_{Y^E} \Bigg/ \sqrt{\sum_{k=1}^{N} \left(\frac{dG}{dY_k}\right)^2\Bigg|_{Y^E}} \qquad (5.23)$$

The normal distance, d, from A to B is

$$d = \frac{G\big|_{Y^E}}{\sqrt{\sum_{k=1}^{N} (dG/dY_k)^2\big|_{Y^E}}} \qquad (5.24)$$

In the space of the original coordinates, Equations 5.22 through 5.24 can be written as

$$x_k^F = x_k^E - \alpha_k \, d \, \sigma_{x_k} \qquad (5.25)$$

$$\alpha_k = \frac{(dG/dx_k)\big|_{x^E} \quad \sigma_{x_k}}{\sqrt{\sum_{k=1}^{N} \left[\left(dG/dx_k\right)\big|_{x^E} \; \sigma_{x_k}\right]^2}} \tag{5.26}$$

$$d = \frac{G\big|_{x^E}}{\sqrt{\sum_{k=1}^{N} \left[(dG/dx_k)\right]\Big|_{x^E} \sigma_{x_k}^{\;\;2}}} \tag{5.27}$$

The point B on the linearized failure surface (Z = 0) may not be a point on the actual failure surface (G = 0). Therefore, consider the failure point, B, as an expansion point. The operations that were performed to reach point B from A, are repeated to obtain point C. Thus, the set of Equations 5.22 through 5.24 are iterated to locate a point on the failure surface (G = 0). The iteration is terminated by setting a criteria as

$$\text{Abs}\ (G\big|_{Y^E}) \leq \delta \tag{5.28}$$

where δ is a specified value. In this study, the first expansion point is taken as the mean values of the random variables. This corresponds to the origin in the transformed space.

The coordinates of the expansion point are determined based on d (Equations 5.24 or 5.27). The expansion point may go out of the solution range if the value of d is too large, and G may not exist at this expansion point. Therefore, the value of d is limited by a step size of h_1, i.e., after every calculation of d, the absolute value of d is compared with h_1. If $|d|$ is greater than h_1, then d is equated to h_1 with the sign of d.

5.4.2. Additional points on the failure surface

The procedure outlined in the previous section, i.e., Section 5.4.1., is used to locate a point on the failure surface, G = 0 (within the iteration tolerance, δ). Let this point be "A" in Figure 19 and its coordinates are represented by Y^F. The values of G and dG/dx_k are used to represent the linearized failure plane, $Z|_A = 0$.

To get a better approximation of the nonlinear G and, thereby, reduce the error between the response failure surface and actual G equal zero surface, several more analyses will be conducted. These analyses will be conducted by locating points near the failure surface, G = 0. To do this, the expansion points are determined along the directions shown in Figure 19. In Figure 19a, the direction Ap_1 is designated as direction 1, because at point P_1 all the variables are at their mean, except the first variable (x_1). Therefore, this direction corresponds to the first variable. Similarly,

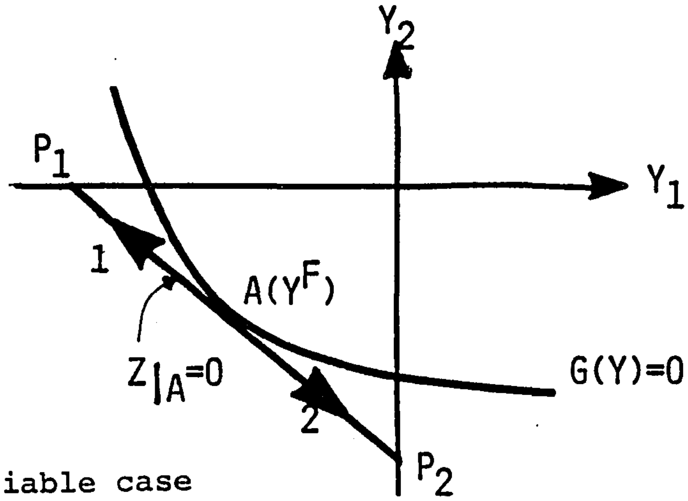

a) Two variable case

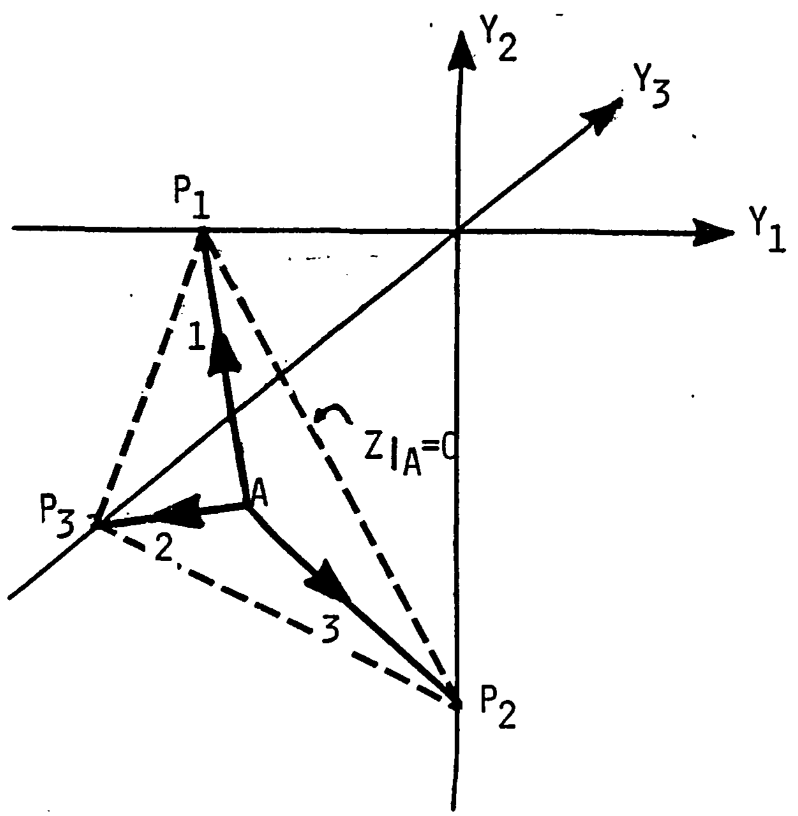

b) Three variable case

Figure 19. Directions for searching failure points

direction 2 corresponds to direction Ap_2. In three variables case (Figure 19b), the expansion points are determined along the directions 1, 2 and 3 which correspond to Ap_1, Ap_2 and Ap_3, respectively. A step size of h_2 is taken in these directions to locate the new expansion points.

For the two variable case, there are only two possible directions for the line $Z|_A = 0$ (Figure 19a). In the case of three variables, the number of directions in the tangent plane, $Z|_A = 0$, is unlimited. For example, in Figure 19b, one could travel in any direction in the tangent plane, $Z|_A = 0$, in addition to Ap_1, Ap_2 and Ap_3. However, only N directions are considered in this study for the N variable case.

Let us consider the k^{th} direction corresponding to the k^{th} variable (Y_k). A distance of h_2 will be traveled in this direction from point A to point B (Figure 20). Point A corresponds to a failure point. Now, point B is chosen for the evaluation of G. Therefore, point B is considered as an expansion point. The coordinates of point B are represented by $\{Y_k^E\}_1$. The subscript k indicates the k^{th} direction; superscript E indicates that it is an expansion point; and subscript 1 shows that it is the first step from the failure point A.

A finite element and gradient analysis is conducted at B. The failure plane is approximated by $Z|_B$ (Equation 5.20). A point on the failure surface, C, is determined. This point is

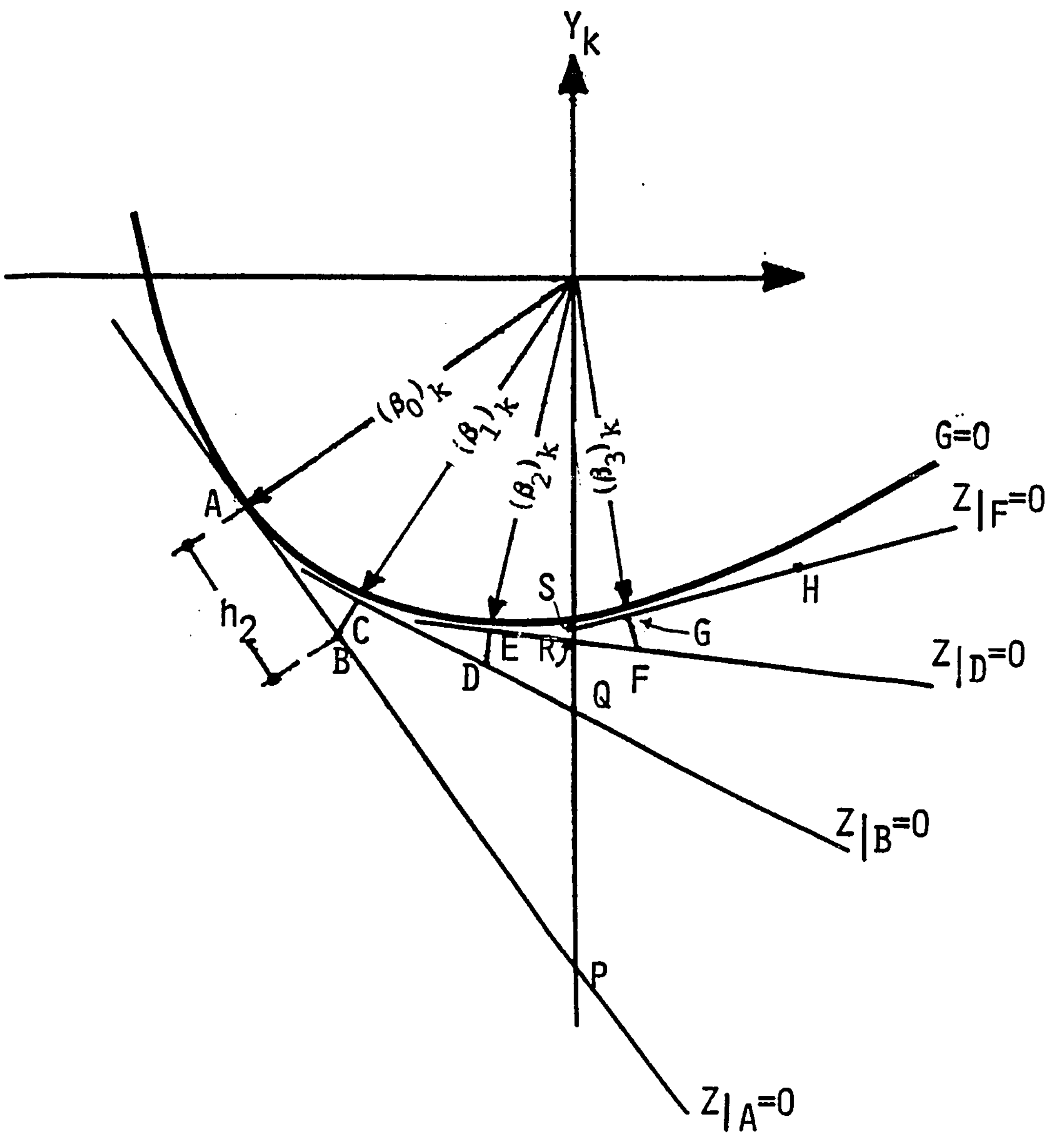

Figure 20. Expansion and failure points in k^{th} direction

at the shortest distance from B to the plane, $Z|_B = 0$. The point C is considered as a failure point. The coordinates of C are determined by the set of Equations 5.22 through 5.24.

Whatever the operations are done to get from A to B and then to C, the same operations are done from C to D and then to E, and E to F to G. The points A, C, E and G correspond to the failure points. Points A, B, D, and F are the expansion points. The total number of steps from A to F are equal to three. This process of obtaining the failure points is done for the remaining k directions, i.e., k is ranged from 1 to N. In each direction, a specified number of steps (NSTEP) is travelled.

The coordinates of the expansion points are

$$\{(Y_k^E)\}_S = \{(Y_k^F)\}_{S-1} + h_2\{\gamma\} \tag{5.29}$$

where S is the step number, h_2 is the step size, and γ is equal to the direction cosines of the vector, v.

$$\gamma_i = \frac{v_i}{\|\{v\}\|} \tag{5.30}$$

and $\|\{v\}\| = \text{Norm of } \{v\} = \sqrt{\sum_{i=1}^{N} v_i^2}$.

The direction vector, v, is given by

$$\{v\} = \left\{ \{(Y_k^{int})\}_S - \{(Y_k^F)\}_{S-1} \right\} \tag{5.31}$$

where $(Y_k^{int})_S$ is the coordinates of an intersection point of the k^{th} variable axis and the plane $Z\big|_{(Y^E_k)_S} = 0$. These points are labeled as P, Q, R, and S in Figure 20. While using Equation 5.31, travel from point G should be in the direction of H and not backwards. In terms of the original coordinates, Equation 5.29 is written as

$$\{(x_k^F)\}_S = \{(x_k^F)\}_{S-1} + h_2 \{Y\} \quad \sigma_{x_k} \tag{5.32}$$

As mentioned before, in each direction, k, the total number of analyses is equal to the specified number of steps. The number of steps is increased if the distance from the origin (mean point) to the failure point is decreased. Specifically, at every failure point, the distance from the origin is determined as (Figure 20):

$$(\beta_S)_k = \sqrt{\sum_{i-1}^{N} \left[(Y_k^F)^2 \right]} \tag{5.33}$$

After taking the specified number of steps in the k^{th} direction, if $(\beta_S)_k \geqslant (\beta_{S-1})_k$, then stop the analysis in the k^{th} direction. If not, consider one more expansion point in this direction (k^{th} variable). This criterion ensures that the approximate linear surfaces cover the region where the failure surface is close to the origin.

5.4.3. Intersection of failure functions

The limit state expressed in Equation 5.1 represents several failure modes. Each mode corresponds to the limitation on the displacement of separate degrees of freedom in the structure. The safe domain is formed by the intersection of these failure functions. For example, let G_1 and G_2 be two failure modes shown in Figure 21. The first analysis is done at the mean values of the random variables and the values of G_1 and G_2 are evaluated. The values of G_1 and G_2 are compared. Note that in Equation 5.1, the values of the Gs are nondimensional. Hence, G_1 and G_2 can be compared. Let the value of G_1 be less than G_2, i.e., $G_1\big|_{Y=0} < G_2\big|_{Y=0}$. Then, consider G_1 to be the active mode, and locate the failure point A on $G_1 = 0$ as explained previously. From point A, a step size of h_2 is traveled to obtain the expansion point B. Then, points C and D are located as failure and expansion points, respectively. At all the expansion points, the values of all Gs are computed and compared. At point D, suppose the failure function G_2 is active, i.e., $|G_2| \leq \delta$. Now, a failure point on the failure surface, G_2, is located (this point is E in Figure 21). Now proceed to point F. Thus, in the case of multiple failure modes, the failure points are determined based on the active failure function.

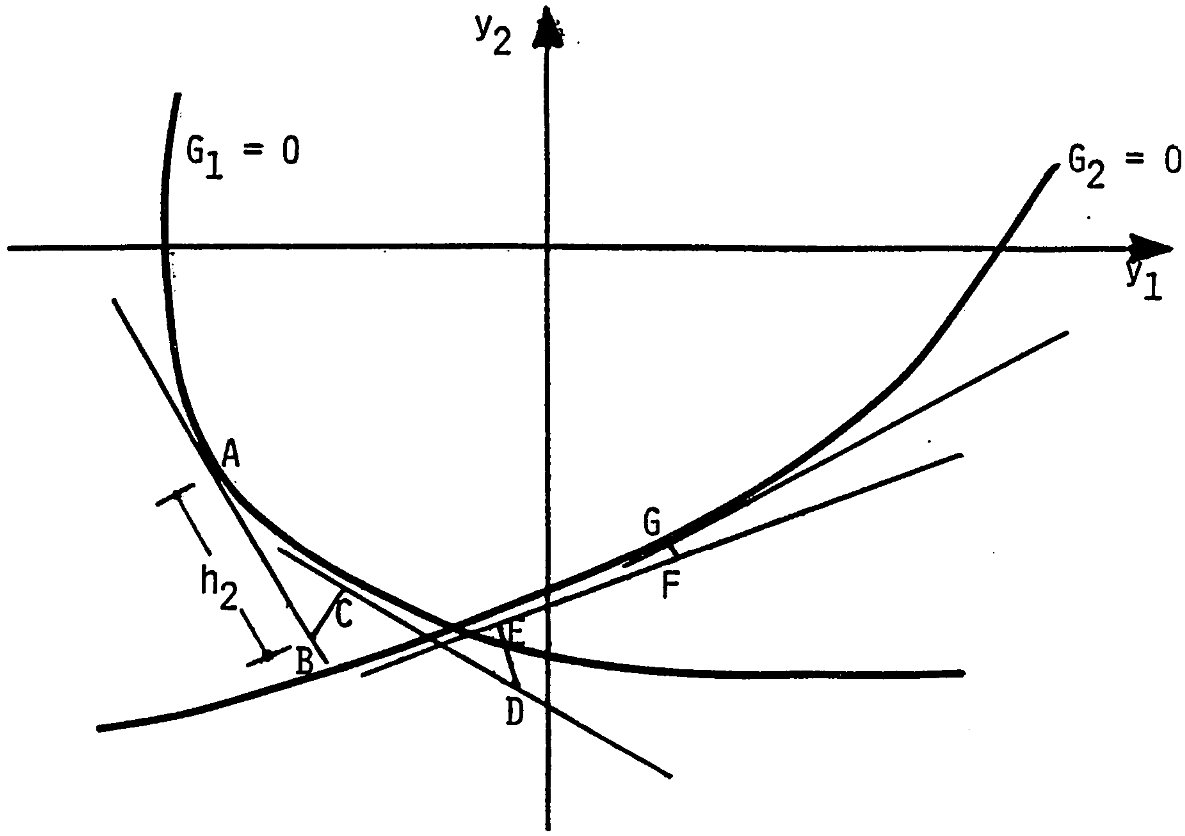

Figure 21. Development of response surface for two failure functions

5.4.4. Response surface expression

After each finite element and gradient analysis, the value of the active G, its gradients, and the coordinates of the expansion points are retained for the formulation of the response surface. At each expansion point, the failure function is expressed by a Taylor's series (Equation 5.20). The safe domain is assumed to be a convex set when the limit state is represented in the form of Equation 5.1 (10, 19). Therefore, the safe domain is bounded by piecewise hyper-planes represented by Zs (Figure 22). For a given set of random variables, the structure is considered to have failed if any one of the Zs predict that G is less than zero. For example, for point P in Figure 22, the value of G calculated from Taylor's series, Z_2, is less than zero. Therefore, point P is considered to be in the failure zone. Note that, according to the response surface, point Q is in the safe domain. Whereas it would actually be in failure region.

5.4.5. Probability of failure

Monte Carlo simulation techniques are used to estimate the probability of failure. This method requires the generation of random numbers by a random number generator. Consider the k^{th} variable. A random number ξ_k is generated between zero and one from a uniform distribution. This number is then used to obtain the value of the random parameter x_k as shown in Figure 23 and by

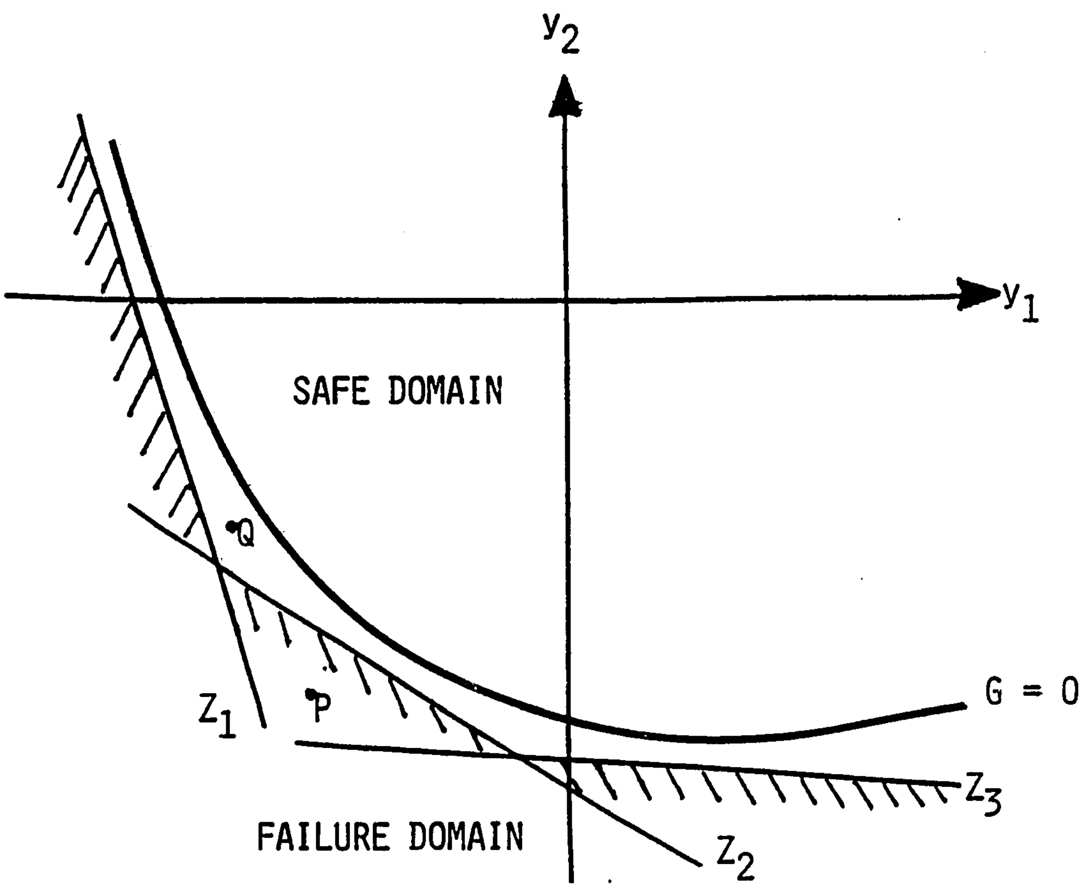

Figure 22. Representation of "safe" and "failure" domain by response surface

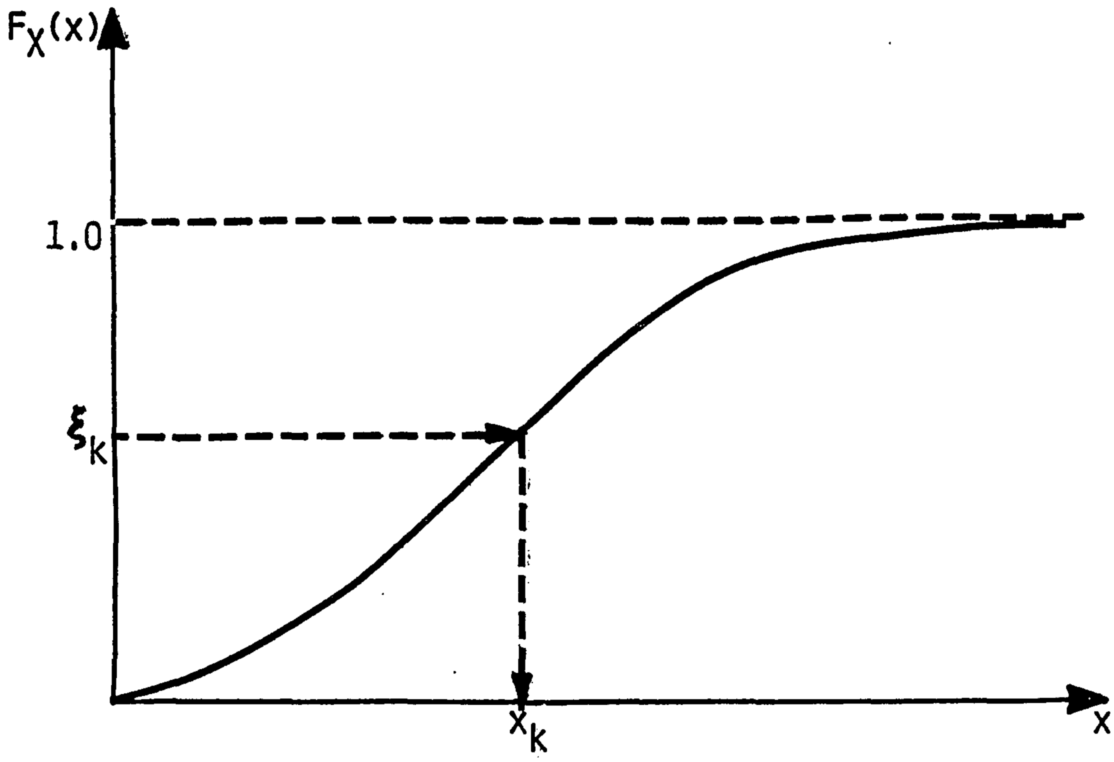

Figure 23. Generation of value of random variables

$$x_k = F_{x_k}^{-1} (\xi_k) \tag{5.34}$$

where F_{x_k} is the cumulative distribution of x_k. Thus, a value for all the random variables is generated.

These values are substituted into the response surface expression (Section 5.4.4.). If the resulting value of G predicted by any one of the Zs is less than zero, the structure is considered to have failed. This procedure of generating the random values for all variables and checking the failure or success is repeated many times (say NS times). The system failure is recorded each time. Let the total number of failures be equal to NF in NS trials. The probability of failure is then estimated as

$$p_f = NF/NS \tag{5.35}$$

The estimate of the probability of failure is exact for an infinite number of trials. For large NS, the sampling distribution of p_f is approximately normal (central limit theorem). Therefore, confidence intervals on the failure probability for a prescribed confidence levels can be determined (17, 28).

5.4.6. Solution procedure

The method explained for obtaining a response surface and conducting the Monte Carlo routine is summarized in this section. The parameters h_1, δ, h_2 and the number of steps (NSTEP) are specified. The number of simulations (NS) in Monte Carlo analysis is also specified.

The algorithm developed in Section 3.5. is used here to perform finite element and gradient analysis. In the algorithm of Section 3.5., the value of the displacement and its gradients are determined. These values are used in finding the value of G (Equation 5.1) and gradients of G (Equation 5.2). The limiting value of the displacements U_{Rj}, are specified. The procedure for the calculation of the failure probability is explained in the following steps.

Step 1. Set the expansion point to the mean value of the random variables, i.e., $\{x^E\} = \{\bar{x}\}$.

Step 2. Perform finite element analysis and gradient analysis (Section 3.5.) at $\{x^E\}$.

Step 3. Compute and compare all G values (Equation 5.1). Let G of j^{th} degree of freedom be the minimum, i.e., $G_j = \mathrm{Min}(G)$.

Step 4. Find the normal distance, d, using Equation 5.27. In the Equation 5.27, the value of G and its gradients correspond to the j^{th} degree of freedom. If the absolute value of d is greater than h_1, then set d equal to h_1*Sgn(d).

Step 5. Find the coordinates of the failure point $\{x^F\}$, using Equations 5.25 and 5.26.

Step 6. Store $\{x^E\}$, $G_j\big|_{x^E}$, and $\{dG_j/dx\}\big|_{x^E}$.

Step 7. If $\left|G_j\right|_{x^E} > \delta$, set $\{x^E\} = \{x^F\}$ and go to Step 2.

Otherwise, proceed to Step 8.

Step 8. Perform finite element and gradient analysis at $\{x^F\}$. Store $\{x^F\}$, $G_j\big|_{x^F}$ and $\{dG/dx\}\big|_{x^F}$.

Step 9. Consider the k^{th} variable. Start with $k = 1$.

Step 10. Let the step number be S, start with $S = 1$.

Step 11. Determine the coordinates of an expansion point, $(x_k^E)_S$, using Equation 5.32. In Equation 5.32, when $S = 1$, $\{x_k^F\}_0$ is equal to $\{x^F\}$. The direction cosine, γ, is calculated using Equation 5.31.

Step 12. Conduct finite element and gradient analysis at $(x_k^E)_S$. Compare all Gs. If G_1 is active, then set $j = 1$. Store $\{x_k^E\}_S$, $G_j\Big|_{(x_k^E)_S}$, and

$\{dG_j/dx\}\Big|_{(x_k^E)_S}$.

Step 13. Determine the failure point $\{x_k^F\}_S$ (Equations 5.25, 5.26 and 5.27).

Step 14. Find $(\beta_S)_k$ using Equation 5.23.

Step 15. If S is greater than or equal to the number of steps (NSTEP) and $(\beta_S)_k$ is greater than $(\beta_{S-1})_k$, proceed to Step 16. Otherwise increment S by one and go to Step 10.

Step 16. If k is equal to the total number of variables N, proceed to Step 17. Otherwise, increment k by one and go to Step 9.

Step 17. Start the Monte Carlo procedure. Set the number of failures, NF, equal to zero.

Step 18. Generate a set of random parameters (Equation 5.34).

Step 19. Substitute these into the response surface expression of Section 5.4.4. If the system is failed, increment NF by one.

Step 20. If the total number of simulations is not equal to NS, go to Step 18.

Step 21. Determine the p_f using Equation 5.35.

5.4.7. Comments

These are the additional comments on the proposed algorithm.

• There is no approximation made for the probability distribution of the random variable. The actual distribution is used in the Monte Carlo procedure.

• The equation for the failure surface is based on the assumption that the safe region is a convex set. Therefore, the response surface is expressed by the intersection of linear surfaces. One could fit a higher degree polynomial through the failure points. However, since the total number of analyses vary depending on the number of steps, the polynomial will be an incomplete one. An arbitrary set of terms would have been included and/or omitted. Also, a system of linear equations must be solved to find the coefficients of the polynomial.

• In the present work, only N directions are considered to create a failure surface. Therefore, the actual failure surface is approximated only in N directions. This is a possible source of error in the estimation of failure probability.

• At the yield point and other structural discontinuities, a small change in the basic variable can cause a large change in the value of the failure function. Therefore, if the step sizes h_1 or h_2 are large, the value of G will be quite large. This may cause some numerical problems.

6. RELIABILITY OF PLANE TRUSSES

6.1. Introduction

The system reliability methods described in the previous chapter are demonstrated in this chapter by application to the plane trusses illustrated in Chapter 4. The probability of failure is evaluated by the following methods.

1. Response Failure Surface Method: This method is developed in this work. The exact limit state is approximated and the Monte Carlo simulation is used to estimate the probability of failure.

2. Advanced First Order Second Moment Method: This method is explained in Section 5.3. The gradients that are required for this method are obtained by the methods of Chapters 3 and 4.

3. Exact limit state method: In this method, the exact limit state expression is used. The Monte Carlo simulation is used to estimate the probability of failure.

6.2. Implementation of Response Failure Surface Method

The solution algorithm for the evaluation of the probability of failure is outlined in Section 5.4.6. This algorithm is implemented in a FORTRAN computer program. In Steps 6, 8 and 12 of Section 5.4.6, the values of G and dG/dx are evaluated by methods described in Chapter 4. To use this program, the following information is needed.

1) Structural Configuration: In a finite element method this is defined by nodal coordinates and element connectivity.

2) Finite Element Properties: For each member, the mean values of the cross-sectional area, yield stress, Young's modulus and the shape parameters of the stress-strain curve must be specified.

3) Loading Specification: The location, direction and magnitude of the nodal loads, as well as the number of load increments, need to be specified. A convergence limit (Section 3.5.) must be specified to stop the iteration in each load step.

4) Random Variable Information: The random variables are described by their probability distribution functions and the parameters of the distributions, such as mean and standard deviation.

5) Limit State Function: To define the limit state function, the limiting displacement of each degree of freedom is read.

6) Response Surface Parameters: The δ value, step sizes h_1 and h_2, and the number of steps in each direction (NSTEP) needs to be specified. These parameters are explained in the previous chapter (Sections 5.4.1. and 5.4.2.).

7) Simulation Parameter: The number of experiments (NS) in the Monte Carlo simulation (Section 5.4.5.).

The result from this program is the number of failures (NF) which is related to the probability of failure (Equation 5.35).

6.3. Example 1: Single Bar Problem

The dimensions and the properties of a single bar are shown in Figure 9. As a first step in this problem, only two random variables are considered. These two variables are the area of cross section of the bar, A, and the yield stress, σ_y, of the material. These two parameters are assumed to be normally distributed with a coefficient of variation of 20 percent. The description of the random variables are given as

$$\begin{aligned} N(\mu_A, \sigma_A) &= N(2.0,\ 0.4) \\ N(\mu_{\sigma_y}, \sigma_{\sigma_y}) &= N(60.0,\ 12.0) \end{aligned} \tag{6.1}$$

where μ_x and σ_x represent the mean and standard deviation of the variable x. A load Q of 40 units is applied at the free end. In the nonlinear analysis, this load is applied in 20 steps. The iterations in each load step is stopped when the norm of the unbalanced force is less than 0.001 (refer to Section 4.5.1.).

To define the limit state, the limiting displacement of the free node is taken as 0.015, or

$$G = 1 - |U|/0.015 \tag{6.2}$$

The bar is considered to have failed if $|U|$ exceeds 0.015. (Note, in all the examples units are not specified. Consistent units are assumed.)

First, the response failure surface method is used. A finite element and gradient analysis is performed at the mean values of the random variables. The value and the gradients of the limit state, G, are evaluated. A step size h_1 equal to 2.0 is taken and a new expansion point is located (Figure 18). If the step size h_1 is taken smaller, more analyses are necessary to reach a point on the failure surface G = 0. The value of δ is taken as 0.05, i.e., iteration to reach the failure surface (G = 0) is continued until the absolute value of G is less than 0.05. Thus, at the failure point, the value of the displacement is between 0.95 (U_R) and 1.05 (U_R). Here, the iteration is carried out until the value of G is equal to 0.034. At this point, the value of the random variable A and σ_y are determined to be 0.967 and 56.63, respectively. This point is considered as the failure point.

The step size h_2 and the total number of steps (NSTEP) in each direction are varied. Note that the step size multiplied by the total number of steps is a measure of the distance travelled from the failure point. Let

$$r = h_2 * \text{NSTEP} \tag{6.3}$$

In the first analysis r is taken as zero, i.e., the number of steps is equal to zero. In this case, the response failure surface is represented by the linear surface expanded at the failure point and by the linear surfaces expanded at other expansion points. The number of simulations in Monte Carlo is set equal to 100,000. The probability of failure is estimated to be equal to 0.00386 (Table 6). Next, a distance of 1.0 (in nondimensional Y-space) is travelled in one step. The p_f is determined to be 0.00449. Then, the step size is reduced by 2 and 4. The converged p_f value is 0.00451. Successively, the value of r is increased to 2.0, 3.0, 4.0, 5.0 and 6.0. In each case, the number of steps are increased. Note that for the case when r is equal to 3.0, and NSTEP is equal to 3, a solution did not exist, that is, the applied load, Q, is greater than the resistance ($A\sigma_y$). In such situations, the step size is decreased and another analysis is carried out. In Table 6, the probability of failure is estimated to be 0.00591 to three significant figures.

The AFOSM method is also used to find the p_f. The minimum distance from the origin to the failure surface in transformed space is determined (Figure 16). This distance is the minimum β and found to be equal to 2.5974. The corresponding p_f is equal to 0.0047 (from Equation 5.12).

In this problem, the exact failure function can be expressed in terms of A and σ_y by using displacement

Table 6. Single bar problem with two variables

r	NSTEP	Step Size (h_2)	NF	p_f=NF/NS
0.0	0	-	386	0.00386
1.0	1	1.0	449	0.00449
	2	0.5	451	0.00451
	4	0.25	451	0.00451
2.0	2	1.0	496	0.00496
	4	0.5	519	0.00519
	8	0.25	519	0.00519
3.0	3	1.0	-[a]	-[a]
	6	0.5	563	0.00563
	10	0.3	568	0.00568
4.0	8	0.5	-[a]	-[a]
	10	0.4	-[a]	-[a]
	20	0.2	588	0.00588
5.0	20	0.25	-[a]	-[a]
	40	0.125	591	0.00591
6.0	60	0.10	591	0.00591

[a]Cases when there was no finite element solution. Step size is too big.

expression of Equation 4.19 in Equation 6.2. This exact expression is used in Monte Carlo simulation of 100,000 trials. This method is referred to as exact limit state method. The probability of failure is estimated to be equal to 0.00591.

The probability of failure from the response failure surface method matches very well with the exact limit state method. The response failure surface method approximates the failure surface by a series of hyper-planes (by lines for the two variable case). Therefore, the nonlinear region is approximated. In AFOSM method, the nonlinear failure surface is approximated by only one hyper-plane. Since the failure domain is convex, the value of the p_f predicted by AFOSM is less than the value estimated by exact limit state method.

Another observation can be made in this example. Suppose the limiting displacement U_R (Equation 6.2) is increased and the probability of failure is again determined. As the value of U_R is increased, the probability of failure is decreased. In Figure 24, the load vs displacement curve and U_R vs the probability of failure is plotted. As U_R is increased beyond 0.05, there is little change in p_f. This is due to the shape of the load displacement curve, which is asymptotic to a horizontal line drawn at a load of 120. Since the failure domain for U_R equal to 0.05 and 0.08 are approximately the

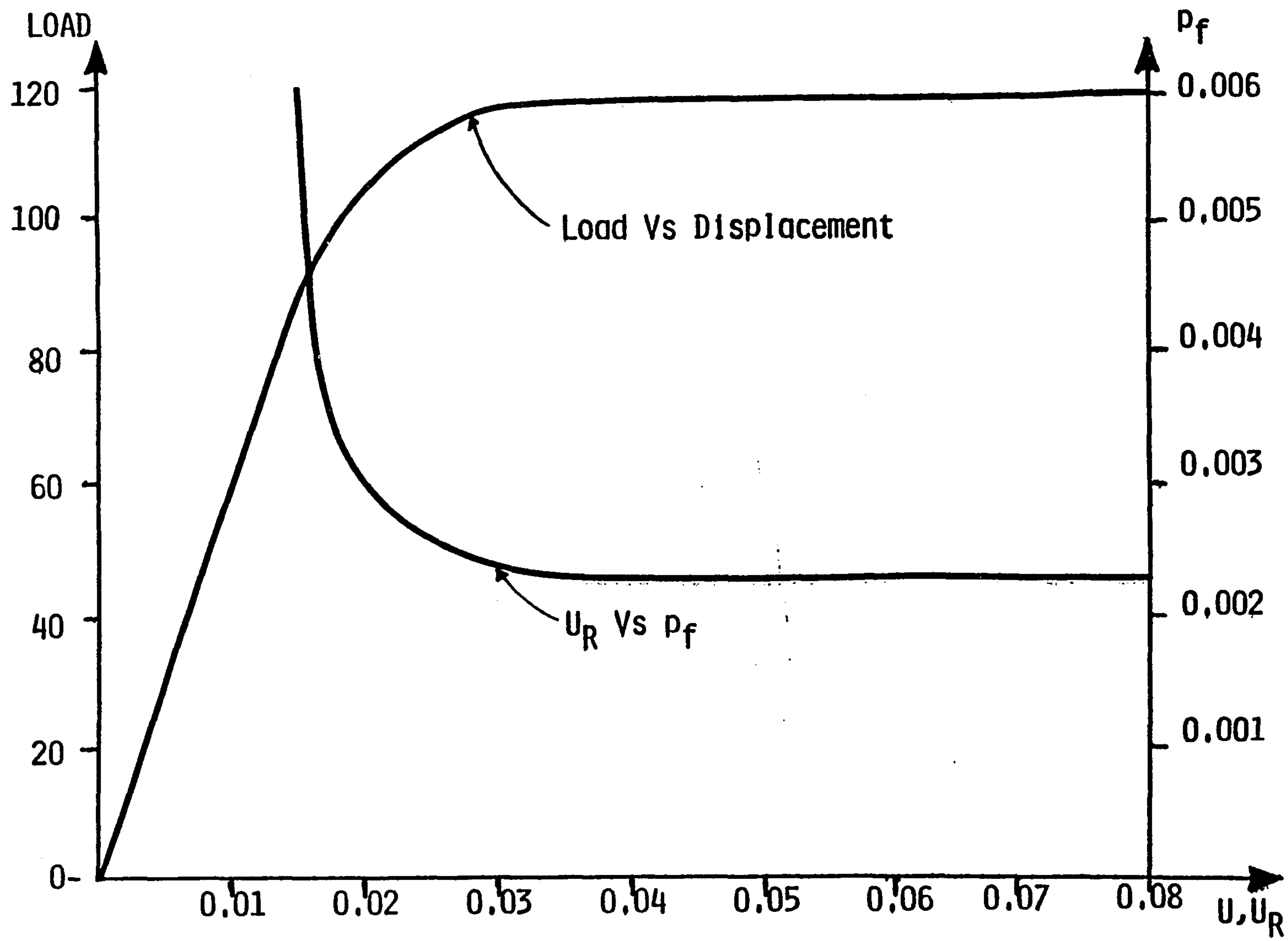

Figure 24. System reliability calculation using displacement limit state

same, the probability of failure for U_R equal to 0.05 and 0.08 is the same and equal to 0.00228.

The system resistance R can be expressed as

$$R = A\sigma_y \tag{6.4}$$

The limit state in terms of the system resistance is expressed as

$$G = R - Q \tag{6.5}$$

A Monte Carlo analysis is carried out using the above equation to estimate the probability that $G < 0$, i.e., $R < Q$. The value is determined to be 0.00228. This numerically confirms the proof presented in Section 5.2. (Equations 5.3 to 5.9) that

$$p_f = Pr(U_Q > U_R) = Pr(R < Q) \tag{6.6}$$

Hence, deflection criteria can be used to estimate the system reliability in terms of load.

This single bar problem is extended to a case of four random variables. The mean values of these variables are shown in Figure 9. All the variables are assumed to be normally distributed with c.o.v.s of 20 percent. The limiting displacement is taken as 0.015. The number of simulations in this case is 20,000.

The response failure surface method is first described. The value of the probability of failure is calculated for different numbers of steps with step size of 0.5 (Table 7). In this case, at an expansion point, the resistance of the structure is less than the applied load, Q, of 40. Therefore, the step is reduced and the number of steps is increased to achieve r of 5. The probability of failure is estimated as 0.0151.

In AFOSM method, the minimum β is found equal to 2.3808. The corresponding probability of failure is 0.008656, Finally, the exact limit state method is used. The exact failure function is expressed by Equation 6.2 where U is given by Equation 4.19. The Monte Carlo simulation is carried out and the estimated probability of failure is determined to be 0.016.

In this case also, the response failure surface method gave comparable results with the exact failure surface method. The discrepancy between these two values can be justified by the fact that the response failure surface is only an approximation to the exact failure function. This observation can be made in the following examples.

6.4. Example 2: Two Bars in Parallel

This example was presented in Chapter 4 to study the gradient analysis method. The geometry, dimensions and the material properties are shown in Figure 11. The area of the cross section (A), Young's modulus (E), yield stress (σ_y), and shape parameter (n) of both members are considered as random

Table 7. One bar problem with four variables

r	NSTEP	Step size (h_2)	NF	P_f=NF/NS
1.0	2	0.5	239	0.001195
2.0	4	0.5	267	0.01335
3.0	6	0.5	295	0.01475
4.0	8	0.5	301	0.01505
5.0	10	0.5	–[a]	–[a]
5.0	20	0.25	302	0.0151

[a]FE element solution did not exist. Step size is too big.

variables. These variables are assumed to have a normal type distribution with a c.o.v. of 20 percent. The mean values are as shown in Figure 11. Also, these variables are assumed to be statistically independent. There are eight random variables in this problem.

A load of 80 units is applied in 20 load steps. To form the limit state function, U_R is specified as 0.015 units. The step size of h_1 is taken as 2.0 and δ as 0.05. The step size, h_2, is taken as 1.0 and the number of steps is increased from 1 to 6. The p_f is estimated for r equal to 6 and step size h_2, equal to 0.5. This p_f is equal to 0.0172.

In AFOSM method, the minimum β is determined to be 2.5091 and the corresponding p_f is 0.006037.

The exact expression for the limit state is derived using the displacement expressions of Equations 4.23, 4.24 and 4.25. This expression is used in a Monte Carlo simulation. The probability of failure is estimated to be equal to 0.02.

A difference in the results of p_f from the above three methods is observed. The value of p_f from the response failure surface method (0.0172) compares well with the result of the exact limit state method (0.02). The difference is small when compared to the difference between the AFOSM method (0.006037) and the exact limit state method. The response failure surface method gives an improved result because the convex failure surface is approximated by many planes,

Table 8. Probability of failure of two bars in parallel

r	NSTEP	Step size (h_2)	NF	p_f=NF/NS
1.0	1	1.0	81	0.0081
2.0	2	1.0	107	0.0107
4.0	4	1.0	139	0.0139
5.0	5	1.0	172	0.0172
6.0	6	1.0	–[a]	–[a]
6.0	12	0.5	172	0.0172

[a]Step size is too big.

whereas in the AFOSM method the failure surface is approximated by only one plane through the design point.

6.5. Example 3: Two Bars in Series

The geometry, dimension and material properties of two bars in series are listed in Figure 12. The statistics of the variables are the same as those in the previous problem. In this case, there are two degrees of freedom. For each of these two degrees of freedom, two failure functions are formulated, i.e., G_1 and G_2. The limiting displacement (U_R) of Node 1 is taken as 0.015 and that for Node 2 as 0.03. The failure functions are written as

$$\begin{aligned} G_1 &= 1 - |U_1|/0.015 \\ G_2 &= 1 - |U_2|/0.03 \end{aligned} \tag{6.7}$$

The limiting displacement, U_R, is selected as 0.015 and 0.03, respectively, in the above equation so as to make both failure modes effective, i.e., comparable probabilities of failure. The value of G_1 and G_2, evaluated at the mean values of the random variables, are equal to 0.555 and 0.424, respectively. According to the algorithm of the response failure surface method, G_2 is considered and a failure point is located on the failure surface $G_2 = 0$. A step size, h_2, of 1.0 is taken from the failure point and response surface is constructed. This response surface is used in a simulation of 10,000 experiments. The p_f is estimated to be 0.0299 (see

Table 9. Probability of failure of two bars in ser[illegible]

r	NSTEP	Step size (h_2)	NF	p_f=NF/NS
1.0	1	1.0	299	0.0299
2.0	2	1.0	356	0.0356
3.0	3	1.0	423	0.0423
4.0	4	1.0	442	0.0442
6.0	6	1.0	–[a]	–[a]
6.0	12	0.5	460	0.0460

[a]Step size is too big.

Table 9). Now, r is increased to 2.0 with the step size of 1.0. The probability of failure is 0.0356. In this case, the failure function G_1 becomes active. For r equal to 6, the probability of failure is calculated as 0.046.

AFOSM method is used to calculate the probability that G_1 and G_2 will be less than zero, independently. The probability that G_1 is less than zero was found in Example 1, as 0.008656. The minimum β corresponding to the second failure mode, G_2, is equal to 2.0083. The corresponding p_f is equal to 0.0223. The bounds on the p_f is constructed using Equation 5.19,

$$0.0223 \leq p_f \leq 0.031$$

The exact limit state (Equation 6.7) can be derived using the displacement expressions of Equations 4.28 and 4.29. These exact limit states are used in 10,000 Monte Carlo experiments and the p_f is estimated to be 0.0605.

In this problem, also, the response failure surface method gave an improved result compared to AFOSM method for the reasons stated previously. Also, in this problem, there are two failure modes G_1 and G_2. In such situations, AFOSM method can only give a bound on the p_f. In the response failure surface method, the intersection of the Gs is accounted for directly at each expansion point based on the active limit state (refer to Section 5.4.3.)

6.6. Example 4: Ten Bar Truss

This problem has been used in the system reliability computations in References 12, 13 and 15. In Chapter 4, this problem was used to study the gradient computations. The structural configuration and material properties are shown in Figure 13. Here, the system reliability of this structure is computed.

The resistance of the members are treated as random variables. The resistance can be expressed by the area of cross section multiplied by the yield stress (Equation 6.4). The yield stress is taken as a deterministic constant of 50 units. The areas of the cross sections are considered as random variables. The mean values of the areas of the cross section and the element resistances are shown in Figure 13. These basic random variables are considered independent, normally distributed with c.o.v.s of 0.2.

The load displacement curve is as shown in Figure 14. In this problem, the system reliability has been expressed in terms of load, i.e., the probability of the load being less than the resistance. The reliability can also be expressed in terms of the displacement limit state (as proved in Section 5.2. and illustrated for a one bar problem in Section 6.3.). The limit state is formulated in terms of the Y-displacement of Node 3. The limiting displacement U_R is taken as 0.032, i.e., the structure is considered to have failed if the

Y-displacement of Node 3 is greater than 0.032. This limiting displacement is based on a trial study similar to the one bar problem (Figure 24). The change in p_f when U_R is increased beyond 0.032 is negligible. Therefore, U_R is taken as 0.032.

The load, Q, is varied and the probability of failure is estimated using the response failure surface. In the nonlinear finite element analysis, the load is applied in 20 steps. Consider the case when Q is equal to 0.5. The value of NSTEP and h_2 are varied, as in previous problems, and the p_f is estimated (see Table 10). The probability of failure is estimated to be 0.0003. Similarly, the p_f is estimated for Q equal to 0.7, 1.0, 1.3, 1.5 and 1.6. For cases when Q is less than 1.0, the number of trials (NS) is taken as 100,000. When Q is greater than or equal to 1.0, NS is reduced to 10,000 because the value of p_f is large for these loads, i.e., a good estimate of p_f can be obtained with fewer simulations. The computer execution times for these problems (NAS 9160 computer) are shown in Table 10. The results for p_f are plotted in Figure 25.

In the AFOSM method the limit state is again associated with the Y-displacement of Node 3. The probabilities of failure corresponding to the different load levels are tabulated in Table 10 and plotted in Figure 25.

In the previous examples, closed form expressions for displacements were available. Therefore, the Monte Carlo

Table 10. Ten bar truss: Probability of failure

	Response Failure Surface Method				AFOSM Method	
Q	CPU in secs.	NSTEP	h_2	P_f	Minimum β	P_f
0.5	140.9	2	0.25	0.00030	3.4998	0.0002326
	263.5	4	0.25	0.00030		
0.7	153.3	2	0.25	0.0010	2.8987	0.001874
	419.0	8	0.15	0.00198		
1.0	90.2	2	0.25	0.0232	1.9962	0.002296
	239.0	8	0.25	0.0382		
1.3	135.4	2	0.25	0.1349	1.0798	0.1401
	186.6	4	0.25	0.1362		
	463.2	15	0.10	0.2572		
1.5	80.1	2	0.10	0.3522	0.4649	0.321
	424.7	15	0.05	0.6164		
1.6	55.7	2	0.10	0.7469	0.1000	0.4602
	106.8	4	0.10	0.7984		
	387.9	15	0.05	0.8210		

analysis using the exact limit state was possible. In this case, a closed form expression for the displacement is not available, which is the case in most practical structures. If the finite element analysis itself is directly used with the Monte Carlo simulation, the amount of computer time will be exorbitant. For example, the execution time for one complete finite element analysis is approximately 0.39 seconds. For 100,000 and 10,000 simulations, it would be 39,000 secs (10.83 hr) and 3900 seconds (1.08 hr) respectively. In Table 10, the execution time taken by the response failure approach is significantly less.

Conducting the FE element analysis NS times can be avoided, however, in this case, since a set of resistance equations given in References 13 and 15 can be used. These resistance equations (R_s) in terms of element resistances (R_i) are given in Table 11. These equations are used to evaluate the probability of failure and plotted in Figure 25. Since the exact limit state is used, these results are referred to as the exact limit state method.

As in previous problems, the results predicted by the response failure surface method are closer to the exact failure surface method than the AFOSM method. However, in this problem AFOSM method gave very reasonable answers in the lower probability range. The computer time taken by AFOSM is approximately 10 times less than the response failure surface

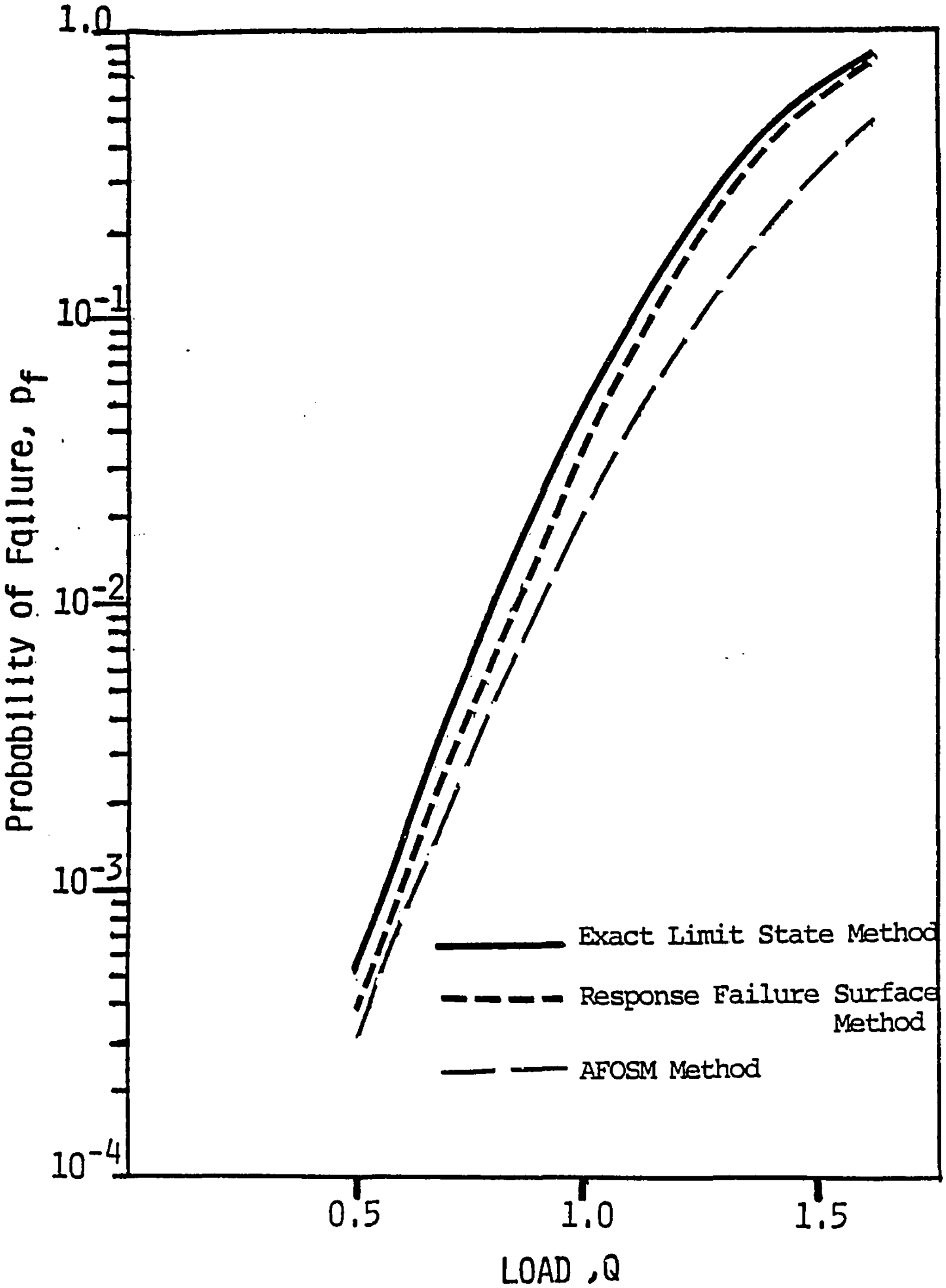

Figure 25. Ten bar truss: Probability of failure vs. load

Table 11. Ten bar truss: System resistance equations

$R_S = \frac{1}{9} R_1$	$R_S = \frac{1}{12} R_4 + \frac{1}{16} R_6$
$R_S = \frac{1}{15} R_7$	$R_S = \frac{1}{8} R_6 + \frac{1}{10} R_8$
$R_S = \frac{1}{18} R_4 + \frac{1}{24} R_5$	$R_S = \frac{1}{6} R_4 + \frac{1}{10} R_8$
$R_S = \frac{1}{16} R_5 + \frac{1}{20} R_8$	$R_S = \frac{1}{6} R_2 + \frac{1}{10} R_9$
$R_S = \frac{1}{15} R_2 + \frac{1}{15} R_4$	$R_S = \frac{1}{5} R_8 + \frac{1}{5} R_9$
$R_S = \frac{1}{9} R_2 + \frac{1}{15} R_8$	$R_S = \frac{1}{8} R_5 + \frac{1}{8} R_6$
$R_S = \frac{1}{12} R_5 + \frac{1}{15} R_9$	$R_S = \frac{1}{4} R_6 + \frac{1}{5} R_9$
$R_S = \frac{1}{9} R_4 + \frac{1}{15} R_9$	$R_S = \frac{1}{3} R_2 + \frac{1}{4} R_5$
$R_S = \frac{1}{6} R_3$	$R_S = \frac{1}{3} R_2 + \frac{1}{4} R_6$
$R_S = \frac{1}{10} R_{10}$	

R_i - Normally distributed

method for the load case of Q equal to 0.5 and NSTEP equal to 2. However, this is a subjective evaluation of the method. The computer time taken by AFOSM can be varied depending on the initial assumed β in the algorithm of Section 5.3.2. If one assumes an initial value of β, which is approximately equal to the minimum β, then the number of iterations will be less and, therefore, the computer time will also be less. For other load cases, the AFOSM method was also about 10 to 15 times faster than response failure surface method.

Although the response failure surface method is expensive compared to AFOSM method, it is much more reasonable than the exact failure surface method. For the case when Q is equal to 0.5 and NSTEP equal to 2, the time taken for each response surface evaluation is approximately 0.000863 seconds. Therefore, out of 140.9 seconds (see Table 10), approximately 86.3 seconds are used for 100,000 evaluations of the response surface expression and the remaining time is used for input, output and finite element and gradient analysis. If we compare this case with the exact limit state method where 39,000 seconds are required, the response failure surface method is orders of magnitude cheaper.

6.7. Discussions

The response failure surface method and the AFOSM methods are used to evaluate the p_f in four examples. In all the examples, an improvement over the AFOSM is obtained by the response failure surface method. The results from the response failure surface methods are comparable with the results using exact limit states. In all the examples, the AFOSM results are less than the response failure surface results. Also, the response failure surface results are less than exact failure surface results. This is because the safe domain is a convex set. In the AFOSM method, the nonlinear region is approximated by one linear surface, whereas in the response failure surface method, the nonlinear region is modeled by several linear surfaces. The computer time taken by each method is discussed in the ten bar problem. The amount of computer time taken by the response failure surface method is reasonable as compared to exact limit state method. More computational effort was needed in the response failure surface method in order to improve the result of AFOSM method.

7. SUMMARY, CONCLUSIONS AND RECOMMENDATIONS

7.1. Summary

System reliability concepts are applicable when the ultimate capacity of the entire structure is of interest rather than only the individual component resistances. For such general structural systems, the overall structural behavior can often be analyzed only by a nonlinear finite element technique. The coupling of reliability concepts with nonlinear finite element analyses for the assessment of system reliability is the topic of this work.

A review of several reliability methods that are developed in the literature is presented in Chapter 2. If these methods are applied to evaluate the system reliability, several shortcomings are encountered. For example, Monte Carlo is computationally expensive. Second order moment methods are difficult to implement when explicit expressions for the limit state and its derivatives are not available. As a result, the improved 2N+1 method, unzipping method, response surface methods and numerical integration methods were developed. However, these methods lack generality, and/or their accuracy decreases at low probabilities of failure. The objective of this work was to develop a system reliability method which can practically be used with finite element analysis.

The objective is accomplished by developing the Response Failure Surface Method. The response failure surface is an approximate failure boundary formed by piecewise hyper-planes. Expressions for the hyper-planes are obtained by finding the values and the gradients of the limit state at several points on the failure surface via finite element analyses. The probability of failure can then be estimated by a Monte Carlo procedure, in which the response failure surface expressions replaces the nonlinear finite element analyses. An evaluation of the response failure surface expression is much cheaper than a nonlinear finite element evaluation. The response failure surface method algorithm is given in Chapter 5.

In the above procedure, the limit state of the system is expressed in terms of a deformation criteria. The Newton-Raphson procedure is used in the nonlinear structural analysis to find the value of the displacement and, thereby, the value of the limit state for a given set of random variables. The matrix equilibrium equations are directly differentiated with respect to the basic variables and solved incrementally to obtain the gradients. The gradient analysis procedure is presented in Chapter 3 and applied for the case of plane truss in Chapter 4. The basic random variables are taken as the cross-sectional area, yield stress, Young's modulus, and shape parameters of the stress strain curve of each truss member.

The gradient analysis algorithm is demonstrated and validated in several examples.

The gradients of the limit state thus obtained are incorporated into the response failure surface method. The gradients are also used in the AFOSM method. With these two methods the probability of failure for the truss examples presented in Chapter 4 are estimated in Chapter 6. In the response failure surface method, the number of hyper-planes that are used to approximate the limit state is increased until convergence in the probability of failure is achieved. In all the examples, the difference in probability of failure between the response failure surface method and exact limit state method is less than the difference between the AFOSM method and exact limit state method.

7.2. Conclusions

The limit state formulated in terms of displacements has the advantage of being able to describe both the serviceability and the ultimate limit states of a structure.

The gradient analysis demonstrated herein for nonlinear structural response has the advantage of being exact (except for truncation and round off errors) and efficient. Efficiency is gained by using the decomposed tangent stiffness matrix from each step of the nonlinear analysis phase to solve for the gradients. The convergence study showed that the gradients of the displacements and stresses have slower rates of convergence than the values of the displacements and stresses themselves. The gradient analysis algorithm presented in this study is general and would be useful in structural optimization and interactive design processes.

The calculated probabilities of failure from the response failure surface method are an improvement over the AFOSM method. The computational cost for the response failure surface method is several times higher than the AFOSM method but considerably less than exact limit state method. The salient advantages of the response failure surface method over the AFOSM method are

1) The response failure surface method is very attractive compared to the AFOSM method for the cases when the failure surface is highly nonlinear. In AFOSM method, the nonlinear failure surface is represented by only one plane, whereas, in the response failure surface method several planes are used.

2) In AFOSM method the nonnormal distributions are approximated by equivalent normal distributions. In the response failure surface method, the actual probability distributions are directly used in the Monte Carlo procedure.

3) The case of several limit states, i.e., several failure modes, is handled directly in the response failure surface method, whereas, in AFOSM method the probability of failure can only be bounded.

7.3. Recommendations

1) The response failure surface method could possibly be made more efficient by using different types of expressions such as polynomials, product form, etc. Additional points on the failure surface could be selected in different directions.

2) The loading parameters and the structural shape (nodal coordinates) should be incorporated as additional random variables.

3) An extension of the gradient analysis and reliability methods could be extended to other types of finite elements.

4) Consideration of geometric nonlinearities in the response failure surface method is a potential area of research.

8. BIBLIOGRAPHY

1. Akin, J. E. Application and Implementation of Finite Element Methods. New York: Academic Press, 1982.

2. Arora, J. S., and Haug, E. J. "Methods of Design Sensitivity Analysis in Structural Optimization." AIAA Journal, 17 (September, 1979), 970-974.

3. Augasti, G., Baratta, A., and Casciati, T. Probabilistic Methods in Structural Engineering. New York, NY: Chapman and Hall, 1984.

4. Construction Industry Research and Information Association (CIRIA). Rationality of Safety and Serviceability Factors in Structural Codes. London, England: CIRIA, July 1977.

5. Cook, R. D. Concepts and Applications of Finite Element Analysis. Second ed. New York: John Wiley and Sons, 1981.

6. Cornell, C. A. "Structural Safety: Some Historical Evidence that it is a Healthy Adolescent." Proc. of ICOSSR 81 and 3rd International Conference on Structural Safety and Reliability, The Norwegian Institute of Technology, June 23-25, 1981. In Structural Safety and Reliability. Ed. T. Moan, and M. Shinozuka. New York: Elsevier Scientific Publishing Company, 1981, pp 19-29.

7. Ditlevsen, O. "Narrow Reliability Bounds for Structural Systems." Journal of Structural Mechanics, ASCE, 7, No. 4 (1979), 453-472.

8. Dolinski, K. "First-Order Second-Moment Approximation in Reliability of Structural Systems:Critical Review and Alternative Approach." Structural Safety, 1 (1983), 211-231.

9. Ellingwood, B., Galambos, T. V., MacGregor, J. G., and Cornell C. A. "Development of a Probability Based Load Criterion for American National Standard A58." National Bureau of Standards Special Publication 577, 1980.

10. Felix, J., and Vanderplaats, G. N. "Configuration Optimization of Trusses Subject to Strength,Displacement and Frequency Constraints." Proceedings of the Second International Computers in Engineering Conference, San Diego, CA. New York: ASME, 1982, pp. 109-118.

11. Froberg, Carl-Eric. Introduction to Numerical Analysis. Second ed. Cambridge, MA: Addison-Wesley Publishing Company, 1969.

12. Gorman, M. "Structural Resistance Moments by Quadrature." Structural Safety, 2, No. 2 (October, 1984), 73-81.

13. Gorman, M., and Moses, F. "Direct Estimate of Structural Reliability." 7 th Conference on Electronic Computation, ASCE, St Louis, MO, August 1979.

14. Greimann, L., and Fanous, F. "Probabilistic Seismic Resistance of a Mark III Steel Containment." Presented at the 1984 Pressure Vessel and Piping Conference, ASME, San Antonio, TX, June 17-21, 1984. In Probabilistic Structural Analysis. Ed. C. Sundararajan. New York: ASME, 1984, pp. 27-39.

15. Greimann, L. F., and Knapp, W. "Reliability Assessment for the Buckling of Stiffened Cylinders." Phase II, Vol. 1. A Report Submitted to Conoco Inc. ISU-ERI-Ames-83284, June 1983.

16. Guenard, Y. F. "Application of System Reliability Analysis to Offshore Structures." Report No. 71. The John A. Blume Earthquake Engineering Center, Stanford University, November, 1984.

17. Hahn, G. J., and Shapiro, S. S. Statistical Models in Engineering. New York, NY: John Wiley and Sons, Inc., 1967.

18. Haldar, A., and Ayyub, B. M. "Practical Variance Reduction Techniques in Simulation." Presented at the 1984 Pressure Vessel and Piping Conference, ASME, San Antonio, TX, June 17-21, 1984. In Probabilistic Structural Analysis. Ed. C. Sundararajan. New York: ASME, 1984, pp. 63-74.

19. Haug, E. J., and Arora, J. S. Applied Optimal Design. New York: John Wiley and Sons, Inc., 1979.

20. Haugen, E. B. Probabilistic Mechanical Design. New York: Wiley & Sons, 1980.

21. Law, A. M., and Kelton, W. D. Simulation Modeling and Analysis. New York: McGraw-Hill Inc., 1982.

22. Leporati, Ezio. The Assessment of Structural Safety. Forest Grove, OR: Research Study Press, 1970.

23. Melchers, R. E., and Tang, L. K. "Dominant Failure Modes in Stochastic Structural Systems." Structural Safety, 2, No. 2 (October, 1984), 127-144.

24. Moses, F. "System Reliability Developments in Structural Engineering." Structural Safety, 1, No. 1 (September, 1982), 3-13.

25. Moses, F., and Rashedi, R. "System Reliability Applications to Offshore Design and Inspection." 4 th ASCE Speciality Conference on Probabilistic Mechanics and Structural Reliability, Berkeley, CA. Ed. Y-K Wen. New York: ASCE, 1984, pp. 103-106.

26. Moses, F., and Stahl, B. "Reliability Analysis Format for Offshore Structures." Presented at the 10 th Annual Offshore Technology Conference, Houston TX, May 8-11, 1978, pp. 29-39.

27. Moses, F., and Yao, T. P. J. "Safety Evaluation of Buildings and Bridges." In The Role of Design,Inspection, and Redundancy in Marine Structural Reliability. Ed. D. Faulkner, M. Shinozuka, R. R. Fiebrandt, and I. C. Frank, Committee on Marine Structures, Marine Board. Washington, D.C.: National Research Council, 1984, pp. 349-385.

28. Neter, J., Wasserman, W., and Whitmore, G. A. Applied Statistics. Boston: Allyn and Bacon, Inc., 1978.

29. Nishino, F., Sato, N., Hasegawa, A., and Inoue, J. "A Probabilistic Basis for Fractile-Based Structural Design." Proc. of JSCE Structural Eng./Earthquake Eng., 1, No. 2 (October, 1984), 135-145.

30. Richard, R. M., and Abbott, B. J. "Versatile Elastic-Plastic Stress-Strain Formula." Technical Note. Journal of Engineering Mechanics, ASCE, 111, EM4 (August, 1975), 511-515.

31. Turkstra, C., and Daly, J. M., "Two Moment Structural Safety Analysis." Canadian Journal of Civil Engineering, 5 (1978), 414-426.

32. U. S. Nuclear Regulatory Commission, "PRA Procedures Guide: A Guide to the Performance of Probabilistic Risk Assessment for Nuclear Power Plants." Report NUREG/CR-2300, September 1981.

33. Vanderplaats, G. N. "Comments on Methods of Design Sensitivity in Structural Optimization." AIAA Journal, 18 (November, 1980), 1406-1407.

34. Vanderplaats, G. N. "Structural Optimization-Past,Present and Future." AIAA Journal, 20, (1981), 992-1000.

35. Vanmarke, E. "Stochastic Finite Element Analysis of Simple Beams." ASCE Journal of Engineering Mechanics, 109, No. 5 (October, 1983), 1203-1214.

36. Wong, S. F. "Uncertainties in Dynamic Soil-Structure Interaction." Journal of Engineering Mechanics, ASCE, 110, No. 2 (February, 1984), 308-324.

37. Yih-Tsuen, Wu, and Wirsching, P. H. "Advanced Reliability Method for Fatigue Analysis." Journal of Engineering Mechanics, ASCE, 110, No. 4 (April, 1984), 536-553.

9. ACKNOWLEDGEMENTS

I wish to express my appreciation to Dr. Lowell Greimann for his guidance and enthusiasm during the preparation of this dissertation. I thank Dr. Fouad Fanous, Dr. Wayne Klaiber, Dr. Max Porter, Professor William Riley, and Dr. Thomas Rudolphi for serving on my graduate committee.

I am especially grateful to my wife, Sunanda, for her continued encouragement and understanding throughout this work.